A VLT/FLAMES survey for massive binaries in Westerlund 1 IV. Wd1-5 – binary product and a pre-supernova companion for the magnetar CXOU J1647-45?

Journal Item

A&A 565, A90 (2014)
DOI: 10.1051/0004-6361/201321771

Astronomy & Astrophysics

A VLT/FLAMES survey for massive binaries in Westerlund 1

IV. Wd1-5 – binary product and a pre-supernova companion for the magnetar CXOU J1647-45?⋆,⋆⋆

J. S. Clark[1], B. W. Ritchie[1,2], F. Najarro[3], N. Langer[4], and I. Negueruela[5]

[1] Department of Physics and Astronomy, The Open University, Walton Hall, Milton Keynes, MK7 6AA, UK
e-mail: s.clark@open.ac.uk
[2] Lockheed Martin Integrated Systems, Building 1500, Langstone, Hampshire, PO9 1SA, UK
[3] Departamento de Astrofísica, Centro de Astrobiología, (CSIC-INTA), Ctra. Torrejón a Ajalvir, km 4, 28850 Torrejón de Ardoz, Madrid, Spain
[4] Argelander Institut für Astronomie, Auf den Hügel 71, 53121 Bonn, Germany
[5] Departamento de Física, Ingenaría de Sistemas y Teoría de la Señal, Universidad de Alicante, Apdo. 99, 03080 Alicante, Spain

Received 25 April 2013 / Accepted 12 March 2014

ABSTRACT

Context. The first soft gamma-ray repeater was discovered over three decades ago, and was subsequently identified as a magnetar, a class of highly magnetised neutron star. It has been hypothesised that these stars power some of the brightest supernovae known, and that they may form the central engines of some long duration gamma-ray bursts. However there is currently no consenus on the formation channel(s) of these objects.
Aims. The presence of a magnetar in the starburst cluster Westerlund 1 implies a progenitor with a mass $\geq$40 $M_{\odot}$, which favours its formation in a binary that was disrupted at supernova. To test this hypothesis we conducted a search for the putative pre-SN companion.
Methods. This was accomplished via a radial velocity survey to identify high-velocity runaways, with subsequent non-LTE model atmosphere analysis of the resultant candidate, Wd1-5.
Results. Wd1-5 closely resembles the primaries in the short-period binaries, Wd1-13 and 44, suggesting a similar evolutionary history, although it currently appears single. It is overluminous for its spectroscopic mass and we find evidence of He- and N-enrichement, O-depletion, and critically C-enrichment, a combination of properties that is difficult to explain under single star evolutionary paradigms. We infer a pre-SN history for Wd1-5 which supposes an initial close binary comprising two stars of comparable ($\sim$41 $M_{\odot}$ + 35 $M_{\odot}$) masses. Efficient mass transfer from the initially more massive component leads to the mass-gainer evolving more rapidly, initiating luminous blue variable/common envelope evolution. Reverse, wind-driven mass transfer during its subsequent WC Wolf-Rayet phase leads to the carbon pollution of Wd1-5, before a type Ibc supernova disrupts the binary system. Under the assumption of a physical association between Wd1-5 and J1647-45, the secondary is identified as the magnetar progenitor; its common envelope evolutionary phase prevents spin-down of its core prior to SN and the seed magnetic field for the magnetar forms either in this phase or during the earlier episode of mass transfer in which it was spun-up.
Conclusions. Our results suggest that binarity is a key ingredient in the formation of at least a subset of magnetars by preventing spin-down via core-coupling and potentially generating a seed magnetic field. The apparent formation of a magnetar in a Type Ibc supernova is consistent with recent suggestions that superluminous Type Ibc supernovae are powered by the rapid spin-down of these objects.

Key words. stars: individual: CXOU J1647-45 – binaries: close – stars: evolution – stars: magnetars – stars: fundamental parameters – stars: abundances

1. Introduction

A major uncertainty in our current understanding of massive stellar evolution is the mapping of initial stellar mass onto supernova (SN) type and the resultant relativistic remnant (i.e. neutron star (NS) or black hole (BH)). The key driver for both relationships is the magnitude of pre-SN mass loss; historically this has been assumed to be mediated by a radiatively driven wind but recently other modes, such as impulsive events and binary mass transfer have received increasing attention.

Three approaches can be taken to resolve this issue (e.g. Muno 2007). First, given the association of a SN remnant with a relativistic object, one can attempt to infer the properties of the progenitor object from the former; a classic example being the Crab nebula (Nomoto et al. 1982). However, this approach is model dependent, with Cas A, for example, being interpreted as originating from both single and binary progenitors of differing masses (Laming & Hwang 2003; Young et al. 2006). Second, theoretical reconstruction of the evolutionary history of (high-mass) X-ray binaries such as GX301-2 (=BP Cru) and 4U1700-37 (=HD 153919) from their current physical properties may be attempted (e.g. Wellstein & Langer 1999; Clark et al. 2002) although once again this methodology is heavily dependant on assumptions made regarding processes such as binary mass transfer.

⋆ Based on observations made at the European Southern Observatory, Paranal, Chile, under programmes ESO 81.D-0324, 383.D-0633, 087.D-0440, and 087.D-0673.
⋆⋆ Appendix A is available in electronic form at http://www.aanda.org

The final approach is to identify relativistic objects within their natal stellar aggregates and hence use the cluster properties to infer the nature of the progenitor. This methodology is challenging. Many compact objects are ejected from their natal association due to SNe kicks; the host association must be demonstrated to be co-eval and in general the properties of the cluster population must be determined via comparison to stellar evolutionary models. Nevertheless, this procedure has been successfully implemented for three clusters, each hosting a magnetar. The brief lifetime inferred for such objects (e.g. $\leq 10^4$ yr; Kouveliotou et al. 1994; Woods & Thompson 2006) implies they should still be associated with their birthsite, hence minimising false coincidences and allowing us to infer that their progenitor was derived from the subset of the most massive stars *currently* present. Moreover, this also allows us to address the parallel problem of determining the mechanism by which the extreme magnetic fields ($B > 10^{15}$ G; Duncan & Thompson 1992; Thompson & Duncan 1993) present in magnetars are generated (Sect. 6). The first two examples identified appear to originate from very different progenitors, with SGR1806-20 evolving from a high-mass star (48^{+20}_{-8} $M_\odot$ star; Bibby et al. 2008)[1] and SGR1900+14 from a much lower mass object ($\sim 17 \pm 2$ $M_\odot$; Clark et al. 2008; Davies et al. 2009). However, in neither case has the cluster Main Sequence (MS) been identified, meaning that progenitor masses have been inferred from post-MS objects via comparison to evolutionary theory, while co-evality has also yet to be demonstrated.

The third association is the magnetar CXO J164710.2-455216 (henceforth J1647-45; Muno et al. 2006a) with the young (~5 Myr) massive ($\sim 10^5$ $M_\odot$) cluster Westerlund 1 (Wd1; Clark et al. 2005)[2]. Unlike the previous examples, its co-evality has been confirmed from studies of both its high- and low-mass stellar cohorts (Negueruela et al. 2010; Kudryavtseva et al. 2012); thus we may safely infer the properties of the magnetar progenitor from the current stellar population. An absolute, *dynamically determined* lower limit to the progenitor mass of J1647-45 is provided by the $23.2^{+3.3}_{-3.0}$ $M_\odot$ + $35.4^{+5.0}_{-4.6}$ $M_\odot$ eclipsing binary Wd1-13 (Ritchie et al. 2010). Given that the current binary period and evolutionary states of both components of Wd1-13 require the lower mass component to have been the initially more massive star, and adopting plausible assumptions regarding pre-SN binary mass transfer (Petrovic et al. 2005), this rises to ~40 $M_\odot$. This in turn is consistent with masses inferred from the spectroscopic classification of the high mass component of Wd1 (e.g. Clark et al. 2005).

Given the expected downwards revision of stellar mass loss rates due to wind clumping (Fullerton et al. 2006; Mokiem et al. 2007) the production of a NS from a >40 $M_\odot$ progenitor appears difficult. However, several theoretical studies suggest that binary driven mass loss can yield such an outcome, even for very massive (~60 $M_\odot$) progenitors (e.g. Brown et al. 2001; Fryer et al. 2002; Yoon et al. 2010). While no stellar counterpart is visible at the location of the magnetar (Muno et al. 2006a) such an absence could plausibly be explained by the disruption of a putative binary at SN. If this were correct, one would expect the companion to have a lower velocity than the magnetar and hence also remain within Wd1. Therefore, the presence of the pre-SN companion is a clear observational prediction of this hypothesis and in this paper we describe the identification and analysis of a potential candidate.

2. Data reduction and presentation

2.1. Radial velocity survey

An obvious prediction for a putative pre-SN companion to the magnetar is that it should have acquired an anomalous velocity with respect to the cluster as a result of the SN, i.e. it should be a "runaway" star (Blaauw 1961).

Various authors have attempted to determine the mean systemic velocity of Wd1 via two distinct methodologies. The first employs observations of neutral H I and molecular material in the vicinity of Wd1 with Kothes & Dougherty (2007) associating Wd1 with the Scutum-Crux arm ($v_{\rm sys} \sim -55 \pm 3$ km s^{-1}) and Luna et al. (2009) with the Norma arm ($v_{\rm sys} \sim -90$ km s^{-1}). However, by their nature they rely on the additional assumption of an association of kinematic and/or morphological features of the interstellar medium with Wd 1 and do not directly sample the velocities of the constituent stars (and hence do not yield a velocity dispersion).

Three additional studies have attempted to measure the velocities of individual cluster members and hence the cluster systemic velocity and velocity dispersion. Mengel & Tacconi-Garmann (2009) employ single epoch observations of 3 red supergiants (RSGs), 5 yellow hypergiants (YHGs) and the supergiant B[e] star Wd1-9 to determine $v_{\rm sys} \sim -53.0 \pm 9.2$ km s^{-1}, while Cottaar et al. (2012) utilise 3 epochs of observations of the luminous blue variable (LBV) Wd1-243 and six YHGs, of which 5 are in common with the previous study, to estimate a velocity dispersion of $\sim 2.1^{+3.3}_{-2.1}$ km s^{-1} (but no systemic velocity determination). However, both studies are hampered by small sample sizes, which comprise stars which are known pulsators and hence radial velocity (RV) variables (cf. Clark et al. 2010), potentially leading to significantly biased RV determinations. Finally Koumpia & Bonanos (2007) make multiple observations of four eclipsing binaries within Wd1 to determine their orbital parameters, from which mean values of $v_{\rm sys} \sim -40 \pm 6$ km s^{-1} are found (or $v_{\rm sys} \sim -45 \pm 14$ km s^{-1} depending on the assumptions made regarding the twin components of Wd1-13).

Between 2008-9 we undertook a multi-epoch RV survey of Wd1, utilising ESO VLT/FLAMES (Pasquini et al. 2002), with the primary goal of constraining the properties of the OB star binary population, but which also permits us to provide a significantly more robust estimate of its bulk kinematic properties (Clark et al., in prep.). Full details of target selection and data acquisition and reduction may be found in Ritchie et al. (2009a). Subsequently, in 2011 we extended this to include the Wolf-Rayet (WR) population (Ritchie et al., in prep.), which also permited the observation of additional OB stars in the spare fibres. Two other configurations were employed encompassing ~20 new stars, with observations made in service mode on 2011 April 17, May 20 and 22 and June 24 with an identical instrumental setup to previous observations[3].

Given the breadth of the emission lines in the Wolf-Rayets, these were excluded from further analysis, as were the pulsationally-prone YHGs and the LBV Wd1-243

[1] The association of 1E 1048.1-5937 with a stellar wind bubble also points to a high-mass (~30–40 $M_\odot$) progenitor (Gaensler et al. 2005).

[2] We also highlight the recent detection of a transient magnetar in the vicinity of the Galactic Centre cluster (Mori et al. 2013). However, as highlighted by these authors, two potential progenitor populations exist in this region, complicating the assignment of a unique progenitor mass for SGR J1745-29.

[3] The GIRAFFE spectrograph operated in MEDUSA mode (HR21 setup), yielding a spectral resolution of ~16 200 between 8484–9001 Å.

(Clark et al. 2010, noting that no blue hypergiants (BHGs) or RSGs were observed). Of the remainder, RVs were determined via Gaussian fits to the line cores of the Paschen series (individually weighted by line strength). Previous model atmosphere analysis of stars in such a temperature regime indicated that significant wind contamination of the Paschen series is only an issue for hypergiants (Clark et al. 2012), giving us confidence in this approach. Unfortunately, the He I photospheric transitions were too weak to be employed for such an analysis for stars of spectral types earlier than B2 (which form the majority of our remaining sample); we note that they are also subject to broadening, which is not included in the model-atmosphere code employed here for such high lying lines (Hillier & Miller 1998, 1999)[4].

This analysis permitted the determination of the systemic velocity of individual objects and hence the cluster as a whole. In order to accomplish this, newly identified pulsators (in addition to the hypergiants) were excluded from further analysis, as were candidate binaries detected via reflex motion but for which orbital solutions could not be determined and those stars with 3 or fewer epochs of observations. This left a total of 61 stars from which we find $v_{\rm sys} \sim -42.5 \pm 4.6$ km s^{-1}; if we also exclude *all* stars which show any indication of binarity in terms of RV variability, spectral morphology, X-ray and/or radio properties (Clark et al. 2008; Dougherty et al. 2010; Ritchie et al., in prep.; Clark et al., in prep.) we are left with a reduced subset of 39 stars that yields $v_{\rm sys} \sim -42.9 \pm 4.6$ km s^{-1}. We regard the velocity dispersion as an *upper limit* given that our limited timebase of observations will not be sensitive to long period binaries.

The unusual emission line BHG Wd1-5 was identified as having a highly discrepant systemic velocity – $RV \sim -99.8 \pm 1.3$ km s^{-1}, or $\sim$−56.9 km s^{-1} relative to the cluster mean – suggestive of a runaway nature. No epoch to epoch RV shifts indicative of reflex binary motion were observed. Informed by the results of quantitative analysis of Wd1-5, we return to a discussion of its runaway nature in Sects. 3 and 5.

2.2. Dedicated observations

Upon the identification of Wd1-5 as a potential runaway we collated existing data to constrain its nature. Photometric data were taken from Clark et al. (2005) and Crowther et al. (2006a) and are reproduced in Fig. 1. Our primary spectroscopic resource were observations made on 2011 May 21 with VLT/FORS2 (Appenzeler et al. 1998). Grisms 1028z (7730−9480 Å), 1200 R (5750−7310 Å) and 1400V (4560−5860 Å) were employed with exposure times of 2 × 60 s, 2 × 600 s and 2 × 980 s respectively. The longslit mode with a 0.3″ slit was used for all observations, yielding a resolution of ∼7000. Data reduction was accomplished following the methodology described in Negueruela et al. (2010). The resultant spectra from both this, our higher resolution VLT/FLAMES run (Ritchie et al. 2009a) and published *JHK*-band observations (Crowther et al. 2006a) are presented in Figs. 2−4; we note that low S/N as a result of interstellar reddening precludes meaningful discussion of the spectrum shortwards of ∼5000 Å.

[4] The missing broadening mechanisms are relevent to the high members of the HeI Paschen-like series ($n \rightarrow 3$) in the *I* band. These members approach hydrogen-like transitions and their theoretical profiles are expected to depart from a pure Doppler profile towards a more Stark-broadened one. Moreover, our current He I atom splits the $L \leq 3$ states only up to $n = 7$, and packs all L states into a single Singlet or Triplet term for $n > 7$. Thus, populations of the high lying HeI levels involved in the *I* band may not be accurately accounted for in our models.

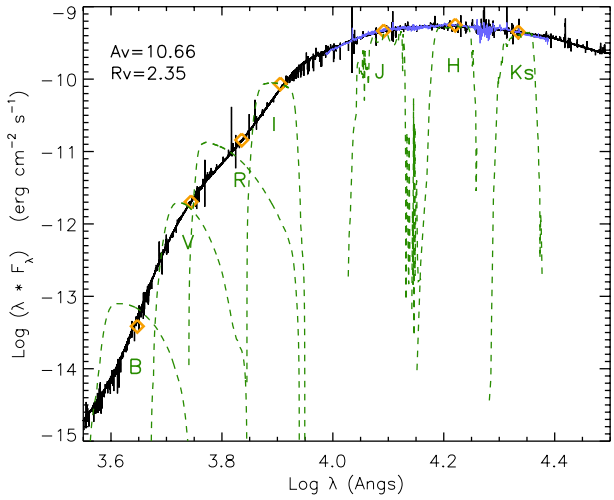

Fig. 1. Comparison of the observed and synthetic spectral energy distributions of Wd1-5. Broadband photometry is given by the yellow diamonds, with the corresponding bandpasses given by the dashed green lines. The observed and synthetic spectra are given by the black and blue lines, respectively.

Wd1-5 shares a similar spectral morphology to Wd1-13 and -44 (Figs. 2−4) and consequently was initially assigned a "hybrid" classification of early-B hypergiant/WNVLh (e.g. Clark et al. 2005). Negueruela at al. (2010) subsequently amended this to B0.5 Ia$^+$, primarily on the basis of the similarity of the *I*-band spectrum to those of the B0.5 supergiants within the cluster; the hypergiant classification being allocated due to the presence of spectroscopic signatures of a high mass loss rate (e.g. strong Hα emission). Note, however, that it is significantly fainter than the cooler (B5-9) hypergiants such as Wd1-33, although comparable to other OB supergiants within Wd1 (Fig. 5). Bonanos (2007) found Wd1-5 to be an aperiodic photometric variable over short timescales but we find no evidence of secular photometric or spectroscopic changes over the past decade (Clark et al. 2010). At other wavelengths Wd1-5 does not appear to support a near-IR excess (characteristic of colliding wind binaries containing a WC star; Crowther et al. 2006a), has a marginal X-ray detection (Clark et al. 2008) and may be associated with a weak, apparently thermal radio source (Dougherty et al. 2010). Thus we find no observational evidence for a binary companion via either direct or indirect diagnostics. In contrast, of the spectroscopically similar stars, Wd-13 is a short-period eclipsing binary (Ritchie et al. 2010) while recent spectroscopy of Wd1-44 suggests a similar conclusion (Ritchie et al., in prep.) and both are rather hard and bright X-ray sources, presumbly due to the presence of shocks in wind collision zones.

Finally we address whether Wd1-5 could be a chance superposition with Wd1. Foreshadowing the following sections, the reddening of Wd1-5 is fully consistent with the mean cluster value (Negueruela et al. 2010). Moreover, both the 8620 Å Diffuse Interstellar Band and the Phillips (2−0) C2 band lines overlapping Pa-12 are identical to other B supergiants in the cluster; furthermore the C2 lines in Wd1-5 also have radial velocities comparable to the cluster mean suggesting the material responsible for the absorption is the same in both cases. The dereddened magnitudes of Wd1-5, the spectroscopically similar stars Wd1-13 and -44 and the OB supergiant population within Wd1 are likewise directly comparable. Indeed, the sole example of an interloper to have been identified, the O9 Iab star HD 151018 ∼2.4 arcmin to south of the nominal cluster centre, is easily distinguished by its discrepant colours and

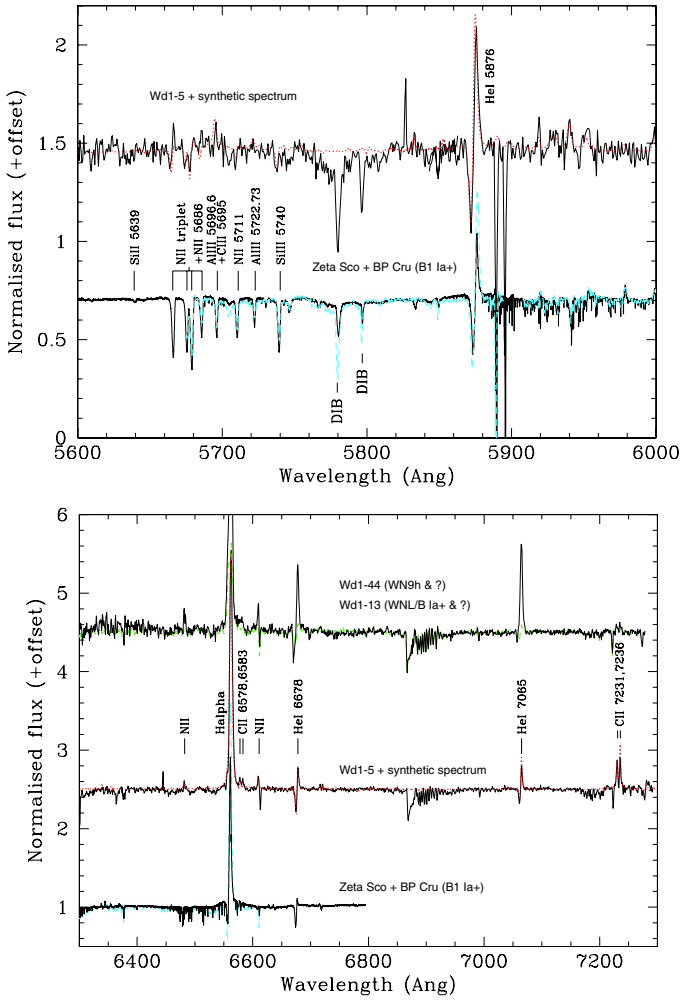

Fig. 2. Comparison of the observed (black, solid line) to synthetic (red, dotted line) spectrum of Wd1-5. Illustrative spectra of selected, closely related early-B hypergiants and WNVLh stars are also shown (with BP Cru and Wd1-13 overplotted in dashed cyan and green lines, respectively, to save space). Spectra of Wd1-13 and 44 were not available in the 5600–6000 Å window, while data on ζ^1 Sco and BP Cru were from Clark et al. (2012) and Kaper et al. (2006). Both Wd1-13 and -44 are SB2 binaries, although a precise spectral classification of their secondaries is uncertain at this time.

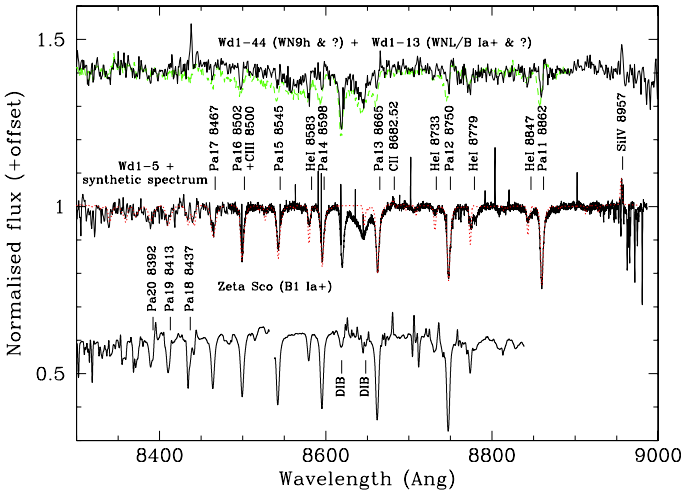

Fig. 3. Continuation of Fig. 2 encompassing the *I* band. Please note the difference in resolutions of the VLT/FORS2 and FLAMES data – the latter plotted longwards of 8475 Å.

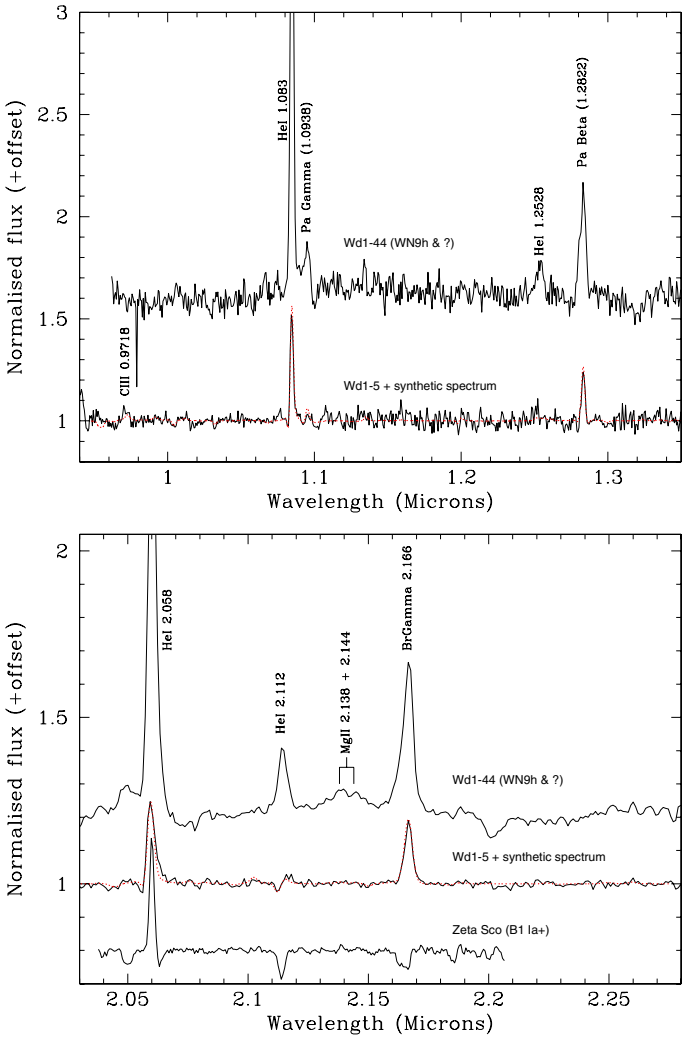

Fig. 4. Continuation of Fig. 2 encompassing the near-IR window (spectra from Crowther et al. 2006a); the spectra are of lower resolution than other wavebands (~1000 versus >7000).

magnitude. Regarding kinematic evidence, we note that under the assumption that Wd1-5 is an interloping field star its radial velocity would place it in an inter-arm void between the Scutum-Crux and Norma arms (Kothes & Dougherty 2007); a less intuitive scenario than the assumption it is a runaway from Wd1. Finally, our quantitative modelling of Wd1-5 (Sect. 3) indicates an anomalous pattern of chemical abudances, which is only replicated in two other Galactic stars and that argues for a specific binary evolutionary pathway consistent with cluster membership (Sect. 4). Given the rarity of such objects, the similarity of Wd1-5 to other cluster members in terms of magnitude and reddening and the explicability of the properties of Wd1-5 in terms of binary evolution as a cluster member, we consider it highly unlikely that it is a distant interloper and hence continue under the hypothesis that it is a runaway star.

3. Stellar properties

3.1. Quantitative modelling

In order to further understand the nature and evolutionary history of Wd1-5 we undertook a quantitative non-LTE model atmosphere analysis of it with the CMFGEN code (Hillier & Miller 1998, 1999), utilising a spectroscopic and photometric dataset

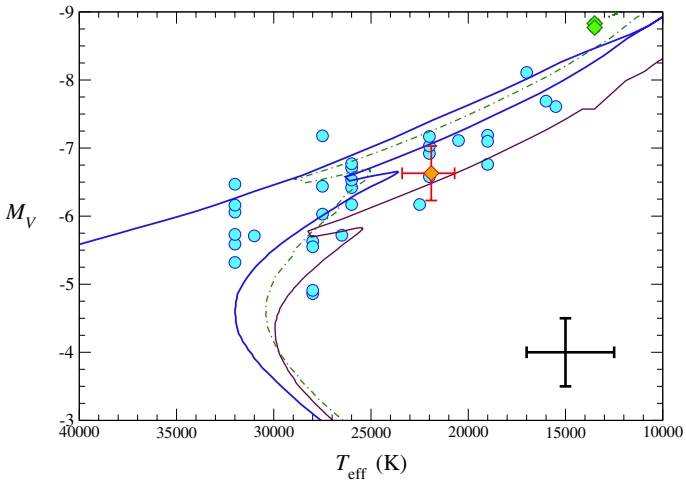

Fig. 5. Semi-empirical HR diagram for Wd1-5 (diamond) and the population of bright OB supergiants (circles) and hypergiants (Wd1-33 and 42; diamonds) within Wd1 (following Negueruela et al. 2010). The solid lines represent the Geneva isochrones (Meynet & Maeder 2000) without rotation for $\log t = 6.7$ (5 Myr; top, blue) and $\log t = 6.8$ (6.3 Myr; bottom, brown). The dash-dotted line is the $\log t = 6.7$ isochrone for high initial rotational velocity. We note that no correction has been made for binary contamination in the sample, which might be expected to contribute to the scatter in absolute magnitudes. Errorbars for Wd1-5 are those quoted in the text, while representative errorbars for the remaining stars are presented in the lower right corner of the plot. These represent typical uncertainties associated with an incorrect assignment of spectral type by ±0.5 subtypes (in $T_{\rm eff}$), and 0.5 mag in M_V to take into account the absolute magnitude and bolometric correction calibrations (as the difference in M_V is negligible between spectral types at Ia luminosity class).

assembled from the above sources. Given the spectroscopic similarity to galactic BHGs such as ζ^1 Sco and BP Cru (Figs. 2–4) we adopted the methodology employed by Clark et al. (2012).

One key result of our analysis is the close proximity of Wd1-5 to the Eddington limit, with $\Gamma \sim 0.9$ being adopted as a *conservative* lower limit (where $\Gamma_{\rm e} \sim 0.52$ is the contribution from electron scattering). Moreover, since the star displays a strong wind, the stellar radius moves towards the wind/photosphere transition region, $R(\tau = 2/3) \sim 0.1 v_{\rm sound}$. These findings imply a sensitivity of the models to the $T_{\rm eff}$ vs. log g pairings and hence particular care was taken in the determination of both parameters.

3.1.1. Temperature determination

To estimate the effective temperature of Wd1-5 and hence constrain the ionisation structure, we made use of several ionisation equilibria, utilizing both Si IV/Si III and C III/C II line ratios simultaneously. The proximity of Wd1-5 to the Eddington limit, together with influence of the wind/photosphere transition region translates into a relatively large uncertainty in our derived value at $T_{\rm eff} = 21\,900^{+1500}_{-1200}$ K (cf. comparable modelling of the early BHGs Cyg OB2 #12, ζ^1 Sco and HD 190603; Clark et al. 2012). This process is shown in detail in Fig. 6, where we display the reaction of the key lines to changes in $T_{\rm eff}$ implied by our estimated uncertainties. In this parameter domain, we found that Si III 5740 Å is extremely sensitive to changes in temperature, while the Si IV 8957 Å line places a firm lower limit. Furthermore, for the high $T_{\rm eff}$ value ($T_{\rm eff} = 23\,400$ K) both the Si IV 6667 Å and 6701 Å transitions should be strongly in emission, but are not present in our data. Similar behaviour is observed in the C III/C II line ratios (see Fig. 6). A high temperature makes the C II 8683Å line vanish and produces excessively strong C III 5695 Å and 9718 Å emission. Likewise, several C III lines, not detected in our spectra, appear in emission (e.g. 5826 Å, 6727 Å and 6515 Å). While no N III and He II lines are detected, N III/N II and He II/He I equilibria may be used as well (see Fig. 6). Many N II lines react strongly to changes in $T_{\rm eff}$, while several N III lines (not detected) appear in emission for the high temperature models (e.g. 6395 Å, 8485 Å and 8572 Å). The He II 10124 Å diagnostic line suffers from poor S/N ratio and spectral resolution; however, from Fig. 6, the high $T_{\rm eff}$ value is clearly excluded.

3.1.2. Surface gravity determination

To estimate log g we made use of the Paschen lines in the high-resolution and signal to noise (S/N) I-band spectrum, as they provide the best constraints for the surface gravity, especially the run of the line overlap among the higher members (see Clark et al. 2012; Fig. 3). The high Paschen lines indeed provide reliable estimates of the stellar surface gravity, as is apparent from Fig. 7, where our current best model together with the upper and lower log g values – $\log g = 2.33^{+0.17}_{-0.10}$ – are compared with the observations. We highlight that low gravity values push the star to the Eddington limit and modify the upper photospheric and transition regions with considerable impact on the lines forming there (lower panels of Fig. 7). Specifically, the lack of emission in N II, Al III, Si III and He II all exclude a lower surface gravity.

3.1.3. Radius and mass determination

Once the effective temperature and gravity were obtained, and assuming a distance of $d \sim 5.0$ kpc to Westerlund 1, we proceeded to fit the observed optical and near-IR spectral energy distribution (SED) of Wd1-5 (see Fig. 1) and hence derived the reddening, stellar radius and, therefore, the stellar luminosity. We used the extinction law from Cardelli (1989). Several tests and comparisons with other laws were carried out, and very good agreement was also found with the latest extinction law from CHORIZOS (Maiz-Apellaniz, priv. comm.). We found $E(B-V) = 4.54$ and a reddening parameter $R_V = 2.35$, corresponding to $A_V = 10.66$. Such a finding is fully consistent with the mean value found for OB supergiants within Wd1 ($E(B-V) = 4.2 \pm 0.4$ with a 1σ standard deviation; Negueruela et al. 2010).

Figure 1 also displays the excellent agreement between our model and the near-IR flux calibrated spectra obtained with SOFI, together with the filters used in the photometry (green-dashed lines). From these values we obtained a stellar radius of $34^{+5.0}_{-4.4}\,R_\odot$, corresponding to a spectroscopic mass of $M = 9^{+4}_{-2}\,M_\odot$ and a final luminosity of $2.39^{+0.78}_{-0.56} \times 10^5\,L_\odot$. We note that the error in the luminosity is dominated by the uncertainty in the reddening determination. Finally, while we strongly favour a distance to Wd1 of ≥5 kpc (Negueruela et al. 2010), a value of 4 kpc (the lower end of literature values) would lead to a revision in radius by a factor of $(d/5\ {\rm kpc}) \sim 0.8$, luminosity by $(d/5\ {\rm kpc})^{1.72} \sim 0.68$ and mass by $(d/5\ {\rm kpc})^{2.0} \sim 0.64$.

3.1.4. Determination of wind properties

Although the moderate reddening affecting Wd1-5 prevents us from securing UV observations from which we might derive firm v_∞ estimates, the dense stellar wind provides alternative v_∞

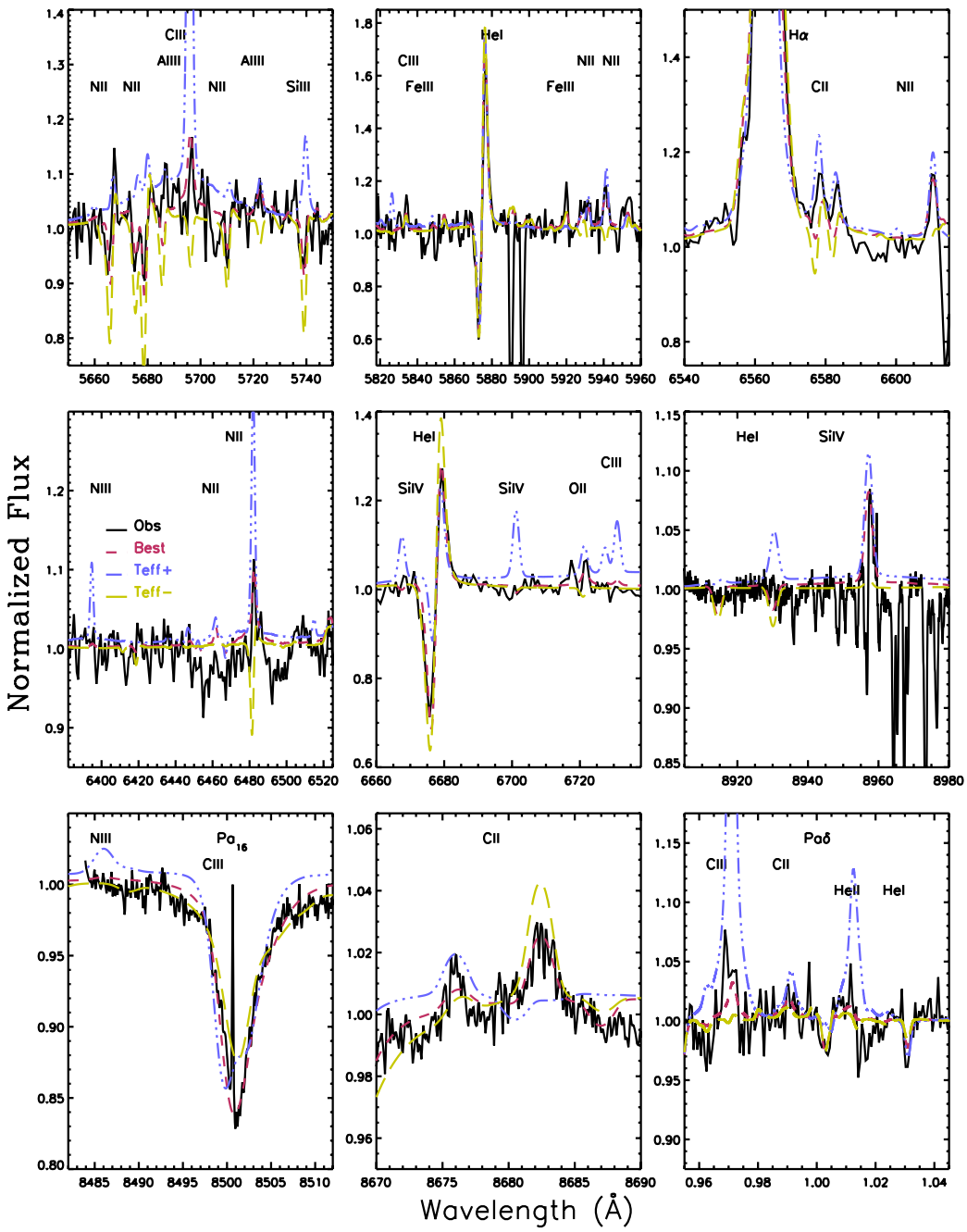

Fig. 6. Determination of $T_{\rm eff}$ for Wd1-5. The best-fit synthetic spectrum is given in red, with spectra utilising the upper and lower error-bounds given in Table 1 presented in blue and green respectively.

diagnostic lines such as Hα, He I 10830 Å and He I 20581 Å. Since the latter two were observed at relatively low (~1000) resolution and moderate (~50) S/N, we basically rely on Hα as primary diagnostic to derive v_∞ and β, the parameter controlling the shape of the velocity field. We obtain $v_\infty = 430^{+20}_{-40}$ km s^{-1} and $\beta = 2.5^{+0.5}_{-0.25}$. The uncertainties are mainly driven by the moderate S/N at Hα due to the reddening.

The main observational constraints which set the mass-loss rate and clumping are the optical Hα, He I 5875 Å, He I 6678 Å and He I 7065 Å lines and the near-IR Paβ, Brγ, He I 10830 Å and He I 20581 Å emission lines. As shown by Najarro et al. (1997, 2006) the latter is extremely sensitive to modelling assumptions and atomic data and is less reliable as an $\dot{M}$ diagnostic; nevertheless, we are still able to reproduce this feature in our synthetic spectrum (Fig. 4). Thus, we were able to derive a mass-loss rate of $\dot{M} = 2.16^{+0.06}_{-0.07} \times 10^{-6}\ M_\odot\ {\rm yr}^{-1}$ (see Table 1) and a clumping factor of $f_{\rm cl} = 0.25^{+0.75}_{-0.15}$. The latter is essentially set by the electron scattering wings of Hα and its error estimates are dominated by the uncertainties in $T_{\rm eff}$ and log g together with the error in the normalisation of the spectra as a result of the S/N in the line. Note that the mass loss scales as $(d/5\ {\rm kpc})^{-1.43}$. We may compare the unclumped $\dot{M} = (2.16/0.25^{0.5}) \times 10^{-6}\ M_\odot\ {\rm yr}^{-1} = 4.32 \times 10^{-6}\ M_\odot\ {\rm yr}^{-1}$ to the theoretically predicted one (Vink et al. 2000). For Wd1-5 stellar parameters we obtain $\dot{M} = 3.0 \times 10^{-5}\ {\rm M}_\odot\ {\rm yr}^{-1}$, a factor of 7 above our value. However, if we just increase our derived mass from 9 to 10.5 $M_\odot$ (a change of 0.07 in log g), the theoretically predicted $\dot{M}$ drops to $\dot{M} = 7.1 \times 10^{-6}\ {\rm M}_\odot\ {\rm yr}^{-1}$ (i.e. just a factor of 1.6 above our value). Thus, we conclude that Wd1-5 may lie in the bi-stability jump region.

Table 1. Model parameters for Wd1-5.

$\log(L_*)$ ($L_\odot$)	R_* ($R_\odot$)	$T_{\rm eff}$ (kK)	$\dot{M}$ (10^{-6} $M_\odot$ yr^{-1})	v_∞ (km s^{-1})	β	$f_{\rm cl}$	$\log g$	M_* ($M_\odot$)	H/He	N/N$_\odot$	C/C$_\odot$	O/O$_\odot$
$5.38^{+0.12}_{-0.12}$	$34.0^{+5.0}_{-4.4}$	$21.9^{+1.5}_{-1.2}$	$2.16^{+0.06}_{-0.07}$	430^{+20}_{-40}	$2.50^{+0.50}_{-0.25}$	$0.25^{+0.75}_{-0.15}$	$2.33^{+0.17}_{-0.10}$	$9.0^{+4.0}_{-2.0}$	$4.0^{+2.7}_{-1.1}$	$9^{+0.15}_{-0.15}$	$1.40^{+0.15}_{-0.15}$	$0.3^{+0.2}_{-0.3}$

Notes. We adopt a distance of ∼5 kpc (Negueruela et al. 2010) and with $A_V \sim 10.66$ (Sect. 3) determine that $M_V = -6.63$ (implying a bolometric correction of −2.1 mag). We note that R_* corresponds to $R(\tau_{\rm Ross} = 2/3)$. The H/He ratio is given by number and other abundances are relative to solar values from Anders & Grevesse (1989); if we use the values from Asplund et al. (2006) as a reference, the derived ratios need to be scaled by 1.38, 1.537 and 1.86 for C, N and O respectively. Finally, our derived H/He abundance corresponds to a surface helium mass fraction, $Y_s = 0.49$.

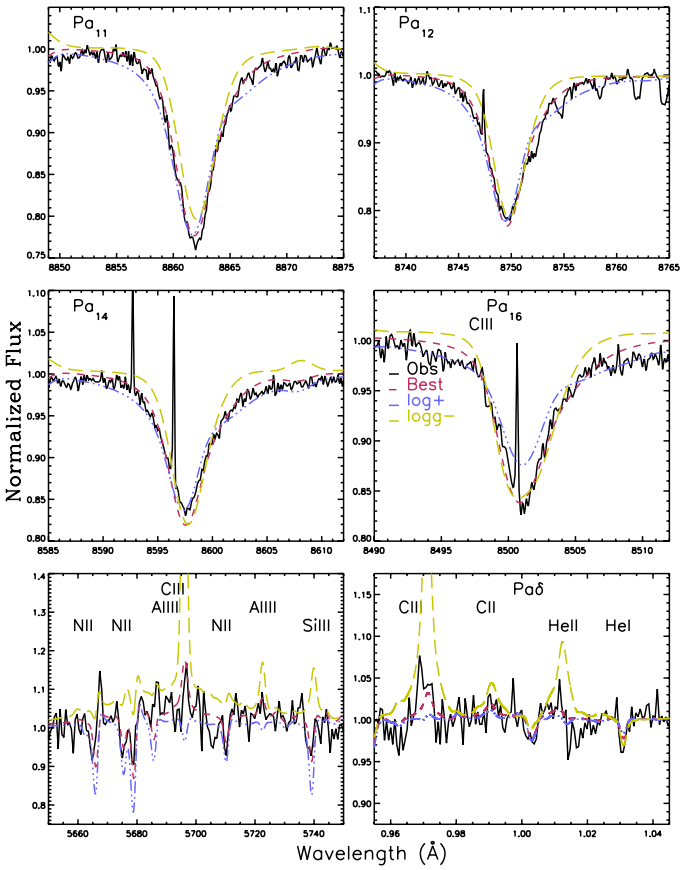

Fig. 7. Determination of $\log g$ for Wd1-5. The best-fit synthetic spectrum is given in red, with spectra utilising the upper and lower error-bounds in Table 1 presented in blue and green respectively.

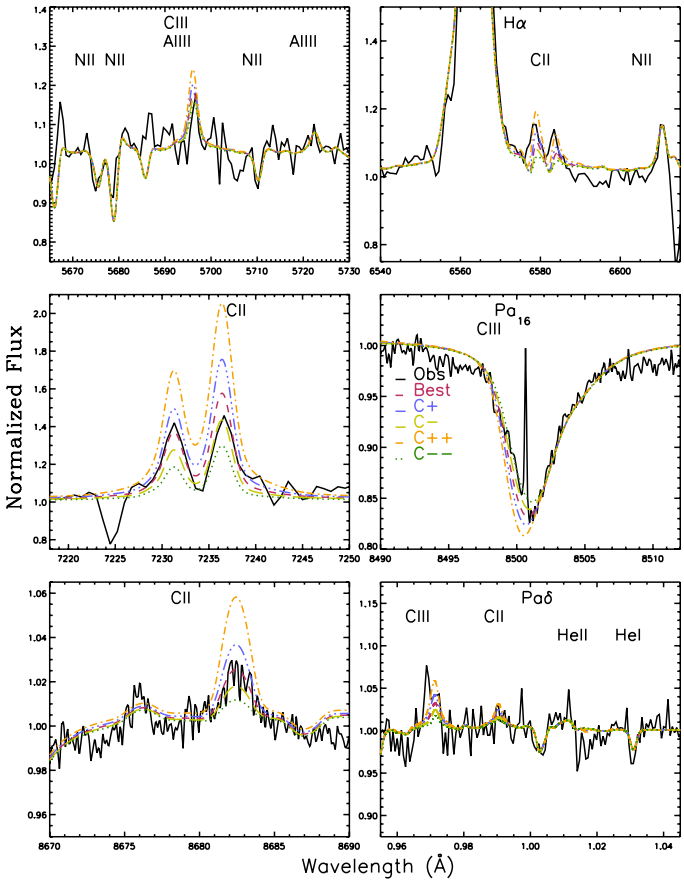

Fig. 8. Determination of the carbon abundance for Wd1-5. The best-fit synthetic spectrum is given in red, with spectra utilising the upper and lower error-bounds given in Table 1 presented in blue and green respectively. Additionally, we provide spectra produced using more extreme, observationally unsupported upper and lower error-bounds (±0.35 dex; orange and dark green respectively).

3.1.5. Abundance determinations

As the derived abundances play a crucial role in our conclusions regarding the nature of Wd1-5, we describe their determination here. In all cases the uncertainties in the abundances take into account the uncertainties in $T_{\rm eff}$ and $\log g$ – i.e. they are estimated considering possible combinations of $T_{\rm eff}$ and $\log g$ within the accepted range. The helium abundance is set by the relative strength of the H I and He I emission lines. We derive He/H = 0.25 by number (49% by mass) with 0.15 and 0.35 as lower and upper limits.

A relatively enhanced carbon abundance (∼1.4× solar) is obtained from the C II 6578−6583 Å, C II 7231−7236 Å and C II 8683−8697 Å lines. The C III 9717 Å and the C II 9904 Å lines present in the low resolution noisy J band spectrum are used as a consistency check. Figure 8 illustrates the sensitivity of the available carbon lines to changes in the abundance. As with Figs. 6 and 7, models labeled as C+/− correspond to changes in ±0.15 dex (our estimated uncertainty), while those labeled as C++/− – have variations of ±0.35 dex in the carbon abundance. The C III line at 5695.9 Å is blended with the Al III 5696.6 Å transition, while the C III 8500 Å line is located within the blue absorption wing of Pa-16, and therefore both are used as secondary abundance diagnostics. The same weighting is given to the C II 6578−6583 Å lines in the red wing of Hα, as they are polluted by the electron scattering emission wing and to C II 8696.7 Å, as it is blended with N II 8697.8 Å. Following from Fig. 8 we therefore estimate an uncertainty of ∼0.15 dex for our derived carbon abundance, confirming the abnormally high value for the present evolutionary stage of the object. We return to this in Sect. 3.2.

The nitrogen abundance is basically constrained from the large number of N II lines throughout the full spectral range covered by our observations. We find a significant enhancement (~9× solar) consistent with moderate CNO processing. Again a value of 0.15 dex should be regarded as a safe estimate for the error in the N abundance. Finally, to derive the oxygen abundance we make use of the weakly detected O II emission lines at 6641 and 6721 Å and the O II absorption lines at 8564 and 8687 Å and obtain a value corresponding to ~0.3 solar. In this case, the uncertainty on the derived abundance is much higher and we obtain 0.2 and 0.3 dex respectively for the higher and lower error estimates.

3.1.6. Additional implications

The close proximity of Wd1-5 to the Eddington limit implies that even moderate rotation may place Wd1-5 close to critical, or breakup velocity ($\upsilon_{\rm crit}$; Langer 1998b; Maeder & Meynet 2000). Utilising the stellar parameters from Table 1 and assuming $\Gamma \sim 0.9$ we may estimate $\upsilon_{\rm crit} \sim 80$ km^{-1}. We obtain an upper limit to the projected rotational velocity of $\upsilon_{\rm rot} \sim 60$ km s^{-1} from the profile of the narrow C II 8683 Å photospheric emission line, which would be consistent with $\upsilon_{\rm crit}$ for inclinations, $i < 49^{\rm o}$; unfortunately we currently have no constraints on the inclination of Wd1-5. In this regard we note that the spectroscopic mass given in Table 1, derived from log$g$ has consequently not been corrected for rotation and hence should properly be regarded as a lower limit; of importance for comparison to the stellar structure scenarios presented for Wd1-5 in Sect. 3.3.

Finally, an important finding from this analysis was that cross correlation of the synthetic to the high-resolution spectrum (~8484–9000 Å) resulted in a significantly lower RV shift of ~−68 ± 4 km s^{-1} relative to rest-wavelength when compared to that determined from Gaussian line-core fitting (~−99.8 ± 1.3 km s^{-1}; Sect. 2.1). We suspect this is due to the presence of excess emission in the red flanks of the Paschen series photospheric lines (due to heavy mass loss), which systematically drives the line centres to shorter wavelengths. Indeed, cross correlation of the spectrum of Wd1-5 to that of a normal supergiant (the BI.5 Ia star Wd1-8b) and a synthetic spectrum of a supergiant of comparable temperature but of higher surface gravity and weaker wind resulted in an RV offset relative to rest-wavelength of over −90 km s^{-1} in both cases. We conclude that the true RV shift of Wd1-5 relative to the cluster mean is smaller than the initial determination of ~56.9 km s^{-1}, but in the absence of an *observational* template, its determination is dependant on the model parameters adopted for the generation of the synthetic spectrum. We therefore adopt a conservative lower limit to the offset from the cluster systemic velocity of >25.1 km s^{-1}; discrepant at the ~5.5σ level with the mean velocity dispersion of stars within Wd1.

Following from the initial discussion regarding the identification of runaways (Blaauw et al. 1961), various studies have refined the criterion for runaway status for 1-dimensional radial velocity data (Vitrichenko et al. 1965; Cruz-Gonzalez et al. 1974; Tetzlaff et al. 2011). These have resulted in a downwards revision in the absolute radial velocity threshold to 25 km s^{-1} and also the adoption of a more generic threshold of $\upsilon > 3\sigma$, where σ is the 1-dimensional mean velocity dispersion of low-velocity stars. Wd1-5 appears to satisfy both criteria, although we note that the former is defined via the motion of field stars within 3 kpc of the Sun (Tetzlaff et al. 2011) and hence there is no a priori reason for this to match the mean velocity dispersion of stars within Wd1.

3.2. Comparison to related objects

In order to place Wd1-5 into an astrophysical context it is instructive to compare its physical properties to those of other galactic BSGs, BHGs, LBVs and Ofpe/WNL (=WN9-11h) stars and related objects. Quantitative analyses of such stars have been undertaken by a number of authors and are summarised in Table A.1. The temperature and radius (and hence luminosity) of Wd1-5 are directly comparable to those of early spectral-type field BSGs; conversely, both BHGs and LBVs appear significantly more physically extended than Wd1-5, which also lies at the high temperature extreme found for these stars. Ofpe/WNLh stars span a wide range of temperatures and luminosities – presumably corresponding to a spread in initial masses – and the temperature and radius of Wd1-5 appears comparable to the least luminous examples, subject to the large uncertainties in these parameters (Table A.1).

Systematic quantitative analysis has yet to be undertaken for the wider population of massive evolved stars within Wd1. Nevertheless, following Negueruela et al. (2010) we may construct a semi-empirical HR diagram for Wd1 (Fig. 5), which demonstrates the close correspondance between Wd1-5 and the cluster OB supergiants, noting that we might expect all these objects to be of similar mass given the co-evality of the population.

Conversely, the wind properties of Wd1-5 do not closely resemble those of either BSGs or Ofpe/WNLh stars, despite similarities in temperature and luminosity. With regard to the former, the wind terminal velocity of Wd1-5 is significantly lower than found for BSGs of comparable spectral type (Fig. 9). In comparison to Ofpe/WNLh stars, both the terminal velocity and mass loss rate of Wd1-5 are at the extreme lower bounds experienced by such stars. A similar discrepancy is found in comparison to the LBVs, which drive slower winds with higher mass loss rates than Wd1-5 (Fig. 9). Indeed, as expected from their spectroscopic similarity, Wd1-5 most closely resembles other BHGs in terms of wind properties, *despite being significantly more physically compact than such stars* (Table A.1). Finally, while we may not readily determine the surface gravity of LBVs and Ofpe/WNLh stars due to the lack of suitable spectroscopic diagnostics, the surface gravity of Wd1-5 appears lower than any of the 20 O9-B0.7 Ia stars sampled in Table A.1, but once again consistent with those found for BHGs.

Therefore, in terms of the combination of both stellar (temperature, radius and surface gravity) and wind (mass loss rate, terminal velocity) properties we are unable to identify a comparable star to Wd1-5, which resembles an OB supergiant in terms of radius but a BHG in terms of surface gravity and wind properties. We return to the implications of these findings in Sect. 3.3.

Lastly we turn to chemical abundances. Both Crowther et al. (2006b) and Searle et al. (2008) assume moderate H-depletion (H/He ~ 4.0) for Galactic BSGs, and find N-enrichment and C- and O-depletion, consistent with the products of CNO burning. Clark et al. (2012) provide a detailed analysis of the abundance patterns of early-B hypergiants. As with BSGs, the three stars studied – Cyg OB2 #12, ζ^1 Sco and HD 190603 – exhibit the products of CNO burning, with carbon being very depleted (C/C$_\odot$ ~ 0.21 ± 0.2, 0.33 ± 0.2 and 0.33 ± 0.2 respectively). This differs from the super-solar abundances we infer for Wd1-5 (C/C$_\odot$ ~ 1.4 ± 0.15) at >5σ level. A similar pattern is also observed for those LBVs for which similar analyses have been performed – C/C$_\odot$ ~ 0.11 ± 0.03, 0.31 and trace for AG Car,

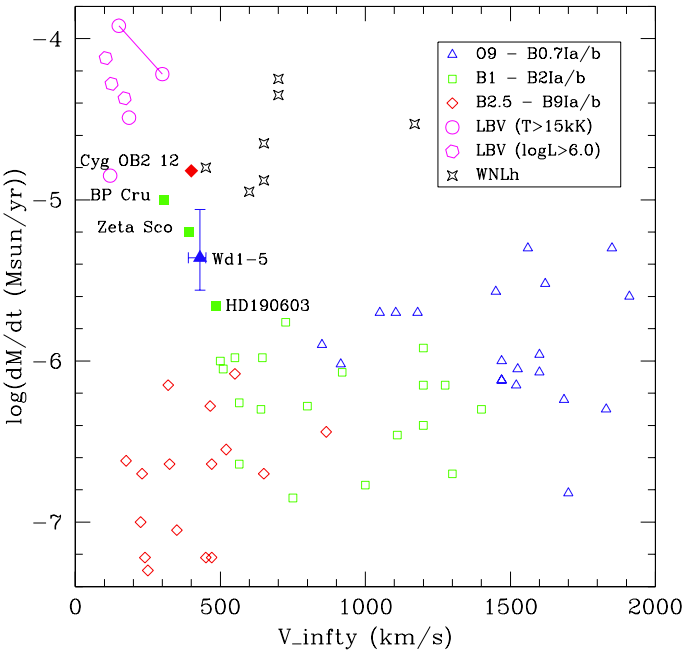

Fig. 9. Comparison of the wind properties of Wd1-5 to field BHGs, BSGs (both plotted according to spectral type, with BHGs given by solid symbols), LBVs and WNLh (=Ofpe/WNL) stars. The data and references employed are summarised in Table A.1. Unfortunately, given the diverse sources employed to construct this figure, it is not possible to plot representative errors for all the objects. In all cases clumping corrected mass loss rates are used to enable direct comparison between individual objects. We estimate $\log \dot{M} \sim -5.36^{+0.3}_{-0.2}$ $M_\odot$ yr^{-1} for Wd1-5 since the errors on the clumping factor in Table 1 are conservative and once this parameter is set the mass loss rate is also determined to a high precision.

P Cygni and Wd1-243 respectively (Groh et al. 2009a; Najarro 2001; Ritchie et al. 2009a).

This behaviour (He and N enhancement and C and O depeletion) is also predicted for single stars by current evolutionary codes (Ekström et al. 2012). Stars of comparable luminosity to Wd1-5 are expected to encounter the BHG phase either side of a red-loop across the HR diagram; prior to this they are expected to exhibit moderately sub-solar ($C/C_\odot \sim 0.2$–0.5) carbon abundances and after this passage they are extremely depleted ($C/C_\odot \sim 0.02$–0.03) due to mass-stripping as a RSG (Jose Groh, priv. comm.).

Therefore, the C-abundance of Wd1-5 is unexpected on both theoretical and observational grounds. We highlight that even in the absence of our quantitative analysis, the evidence for a high C-abundance is compelling; simple comparison of the optical spectra of Wd1-5 to the two other cluster BHG/WNLh stars – Wd1-13 and -44 – reveals the anomalous strength of the C II 7231 Å and 7236 Å lines in Wd1-5, with these lines being essentially absent in its spectroscopic twins (Fig. 2). All three stars are expected to share the same natal metalicity and evolutionary pathway (since Wd-1 appears essentially co-eval; Negeuruela et al. 2010; Kudryavtseva et al. 2012) and so it is difficult to account for this observational finding unless Wd1-5 has a greater C-abundance than these objects.

To date, the sole exceptions to these abundance patterns are the B1 Ia$^+$ hypergiant BP Cru (=Wra977) and the O6.5Iaf$^+$ star HD 153919; the mass donors in the high mass X-ray binaries GX301-2 and 4U1700-37 respectively. In addition to the expected He- and N-enrichment, both show significant C-enrichment over CNO equilibrium values ($C/C_\odot \sim 2$ and 1 respectively; Kaper et al. 2006; Clark et al. 2002) in an analagous manner to Wd1-5; the implications of this finding are discussed below.

3.3. Internal structure and evolutionary state

Given the discrepancies in the properties of Wd1-5 when compared to other massive evolved stars we may also employ our quantitative analysis to try to determine the internal structure – and hence evolutionary state – of Wd1-5 via comparison to theoretical predictions. An immediate difficulty is encountered when attempting to reconcile the high intrinsic luminosity with the spectroscopic mass estimate, in the sense that it appears significantly overluminous for a star of normal composition. If Wd-1 were found at a lower distance than the 5 kpc adopted here this discrepancy becomes worse in the sense that stellar mass decreases more rapidly as a function of distance than luminosity does. Thus, while the absolute masses of the models described below would be reduced, our qualitative conclusions would remain entirely unchanged.

In order to replicate our modelling results we investigated three different scenarios to overcome this limitation:

Scenario (i): Wd1-5 is chemically homogeneous. From Eq. (11) of Graefener et al. (2011) we derive $M = 32.5$ $M_\odot$, leading to $\log g = 2.79$, $\Gamma_e = 0.168$, and an escape velocity, $v_{\rm esc} = 520$ km s^{-1}.

Scenario (ii): Wd1-5 is core-helium burning and possesses a shallow H-envelope. From Eq. (18) of Langer (1989a) we find $M = 13.7$ $M_\odot$, resulting in $\log g = 2.41$, $\Gamma_e = 0.40$ and $v_{\rm esc} = 290$ km s^{-1}.

Scenario (iii): consisting of a hybrid of the above, whereby Wd1-5 has burnt hydrogen in the core to the stage of $X_{\rm core} = 0.1$. and has little envelope mass. Then we may again employ Eq. (11) of Graefener et al. (2011) to determine $M = 18.6$ $M_\odot$, $\log g = 2.54$, $\Gamma_e = 0.30$, and $v_{\rm esc} = 360$ km s^{-1}.

Scenario (i) appears excluded on the basis of pronounced discrepancies between the predicted and observed values of $\log g$ (and hence stellar mass), wind velocity ($v_{\rm esc}$ versus v_∞) and $\Gamma_{\rm e}$. However, scenarios (ii) and (iii) – that Wd1-5 is essentially an He-star with relatively shallow H-envelope – appear more acceptable in terms of these properties. In such a picture v_∞ exceeds the predicted $v_{\rm esc}$, as might be expected and $\Gamma_{\rm e}$ approaches the value of 0.5 determined via modelling, noting that for Galactic metallicities, the Eddington factor based on the full Rosseland mean opacity in the atmosphere of hot massive stars is larger by ~0.3 compared to the case when only electron scattering is considered as an opacity source. Likewise, the discrepancy between predicted and spectroscopic masses (Table 1) may be ameliorated by the inclusion of the (uncertain) correction due to the effects of stellar rotation, given the proximity of Wd1-5 to the Eddington limit (Sect. 3.1).

Nevertheless, if Wd1-5 were born with a mass at the main sequence turn-off of Wd1 (~40 $M_\odot$; Ritchie et al. 2010), we would find it difficult to account simultaneously for the luminosity of Wd1-5 and the observed, He-rich surface chemistry under the assumption of mass loss driven by stellar winds (Brott et al. 2011). Moreover, we would not expected it to achieve such

an apparently low mass while retaining such a high hydrogen content. Conversely, while the current mass would be explicable if Wd1-5 was born with a lower initial mass (~20 $M_\odot$), we would not expect such a star to have evolved from the main sequence given the current age of Wd1 (Negueruela et al. 2010). Furthermore, the requirement for stellar winds to yield the observed surface chemistry would be even more implausible.

As well as He-enrichment, Wd1-5 is also N- and, critically, C-enriched. Unlike the He- and N-enrichment, which in principle might be understood as the result of products of the CNO cycle being transported to the surface via rotational mixing, the C-enhancement over CNO equilibrium values *cannot* arise from such a mechanism, since any carbon produced by He-burning would have to pass through overlying H-burning layers prior to reaching the surface where it would be converted into nitrogen (e.g. Clark et al. 2002). Consequently, this cannot be the result of the evolution of a single star and must be the result of mass-transfer from a C-rich bianry companion.

Therefore, in order to reconcile the luminosity, mass and surface composition, we are forced to conclude that Wd1-5 must have been subject to an additional source of mass-loss, which we suppose was binary-induced, since we also must infer (subsequent) mass-transfer from a putative binary companion.

4. The nature and formation of Wd1-5

4.1. A pre-SN binary evolutionary pathway

At first glance, the dual requirements of binary driven mass loss and gain required to explain the abundance pattern of Wd1-5 appear contradictory. Nevertheless we believe they may both be accomodated in a single evolutionary scheme, which we describe here. We first consider the mass loss mechanism responsible for the removal of the majority of the H-mantle of Wd1-5. Case B and case C mass transfer would have quickly yielded unacceptably high surface He-abundances (e.g. Y_s = 0.8 in 10^4 yr for case C), which would have subsequently increased very quickly, resulting in a low likelihood of catching Wd1-5 in its current state. Conversely, while case A mass transfer also produces stars with He-abundances comparable to that of Wd1-5, crucially the state persists for a significant fraction of the stellar lifetime (~10^6 yr; Fig. 10, following Wellstein & Langer 1999); we therefore conclude that Wd1-5 likely evolved via case A evolution.

The requirement for the mass-*gainer* to both avoid merger and explode first to unbind Wd1-5 places important constraints on the pre-SN system. Assuming a ~41 $M_\odot$ primary (Ritchie et al. 2010), a rather massive companion is required to avoid merger during the binary interaction, but even in a $M_{\rm init}$ ~ 41 $M_\odot$+ ~ 30 $M_\odot$ system – as suggested for the eclipsing BHG/WNLh+O supergiant binary Wd1-13 (Ritchie et al. 2010) – we would still expect the initial primary and mass donor to undergo SN first, despite the companion accreting significant quantities of matter. This behaviour results from the fact that the evolution of the mass-gainer is rather sensitive to the assumed timescale for semiconvective mixing; while the mass-gainer attempts to increase its convective core mass in response to the accretion of material, this rejuvenation process is hindered by the chemical barrier imposed by the presence of (accreted) H-rich matter on top of He-rich material (see Braun & Langer 1995). However, if the initial mass ratio of the putative binary system instead approached unity, a reversal of the supernova order would be expected (Wellstein et al. 2001), while rejuvenation of the mass gainer would still not occur. We note that such a mass ratio would not be expected to affect the case A evolution of the mass donor, which would still evolve into the same He-rich overluminous state that we currently find Wd1-5 to be in.

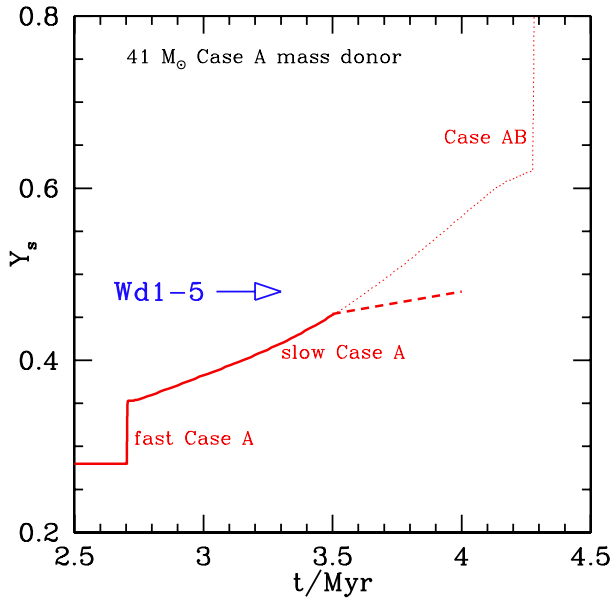

Fig. 10. Evolution of the helium abundance of a 41 $M_\odot$ primary in an initial 6 d orbital period massive binary under the case A evolutionary scenario described in Sect. 4.1, where mass loss and He-enrichment is driven by both stellar wind and binary induced mass transfer (solid red line). The dashed line represents our prediction of the evolution of Wd1-5 in a post-common envelope phase, whereby only stellar wind mass loss is present; for completeness the dotted line represents the continuation of the specific evolutionary model of Petrovic et al. (2005) if a common envelope had not formed. Finally, a brief episode of wind-driven reverse mass transfer during the pre-SN WC phase of the companion star accounts for the anomalous C-rich chemistry of Wd1-5.

So, we might suppose an hypothetical binary initially comprising two ~41 $M_\odot$ + 35 $M_\odot$ stars – where the more massive component represents Wd1-5 – in a compact (initial orbital period $P_{\rm init}$ < ~8 d) configuration in order to permit case A mass transfer. Following the approach of Petrovic et al. (2005), such an evolutionary pathway would lead to the 41 $M_\odot$ primary losing ~20 $M_\odot$ by t ~ 3.5 Myr during fast case A mass transfer, corresponding to the fast rise in Y_s at that time (e.g. system #4 of Petrovic et al. 2005; Fig. 10). The original secondary accretes a sizable fraction of this material and becomes a ~55 $M_\odot$ star. Because it is so luminous as a result of this process and as it does not rejuvenate, it finishes core H-burning well before the donor star does (i.e. before t = 4.25 Myr). During the remaining core H-burning stage of the mass-gainer, the system is of Algol type, meaning that the mass-donor (corresponding to Wd1-5) fills its Roche lobe and undergoes slow case A mass transfer. During that phase, the surface helium abundance subsequently rises from about Y_s = 0.34 to a value of up to Y_s = 0.47; in excellent agreement to that found for Wd1-5 (Sect. 3.1).

Petrovic et al. (2005) showed that the mass-gainer is significantly spun-up by such an accretion process. In their 56 $M_\odot$ + 33 $M_\odot$ system, the mass-gainer subsequently spins down again after accretion due to its long remaining core hydrogen burning life time after rejuvenation. In our case, with a mass ratio close to 1 and without rejuvenation, the mass-gainer is not likely to have the time to do so, but will instead keep a high specific angular momentum until core hydrogen exhaustion.

When the mass-gainer finishes core H-burning, the quantitative predictions of the model end. The mass-gainer will certainly

expand after core H-exhaustion and, with an orbital period in the ~10−20 day range, it will interact with Wd1-5, likely engulfing it. While one would typically expect such interaction to lead to merger, we emphasise that the mass (~55 $M_{\odot}$) and hence luminosity of the mass-gainer will be so high that its envelope will approach the Eddington limit and hence be only lightly bound. Therefore we suggest that both stars survive this phase, with the H-rich mantle of the mass-gainer ejected in a LBV/common envelope phase analagous to those driven by the RSG phase in lower mass systems as the orbital period of the binary decreases. This process will result in its transition to a WR state. Unfortunately, current simulations of binary evolution do not include such a phase due to the complexity of the physics. However, in support of this assertion we emphasise that the current configurations of the high-mass X-ray binaries 4U1700-37 and OAO 1657-415 also require the occurrence of exactly such a process in systems containing stars too massive to pass through a RSG phase (Clark et al. 2002; Mason et al. 2012); demonstrating that such a scheme is indeed viable and has observational precedents.

Subsequently, due to the short period of our binary – and guided by the evolution of the analagous pre-SN binary progenitor of 4U1700-37 (Clark et al. 2002) – we might expect pollution of the atmosphere of Wd1-5 by the carbon-rich stellar wind of the pre-SN WC phase of the mass-gainer; this representing the second phase of (reverse) wind-driven mass transfer required to yield the observed surface abundance pattern of Wd1-5. Approximately 0.05 $M_{\odot}$ of carbon would be required to have been accreted to replicate the current chemistry[5]; hydrodynamical simulations (Dessart et al. 2003) suggest such a process is possible and it indeed appears to have occured in 4U1700-37, despite the more powerful wind of the recipient in this system (HD 153919; Clark et al. 2002). Finally, the WC mass-gainer will explode as a Type Ibc SN and will likely unbind the binary. The absence of rejuvenation during the case A accretion and the subsequent early exposure of the core results in a sufficiently low pre-SN iron core mass to form a NS rather than a BH (e.g. Fryer et al. 2002). We explore this phase of the binary evolution in more detail in Sects. 5 and 6.

4.2. Evolutionary pathways for massive stars in Wd1

Building on the evolutionary schemes delineated in Clark et al. (2011) we might suppose an additional pathway for close binaries comprising two stars of comparable masses, such that for stars within Wd1 current evolving from the MS ($M_{\rm init}$ ~ 35−50 $M_{\odot}$):

> *Case A binary, similar masses*: O6-7 V (primary) + O6-7 V (secondary) → case A mass transfer → BHG/WNLh + O III-V → BHG/WNLh + LBV → LBV/common envelope evolution → BHG/WNLh + WN/WC (+ wind driven mass transfer) → SN + binary disruption → BHG/WNLh + magnetar/NS.
> *Case A binary, disimilar masses*: O6-7 V (primary) + OB V (secondary) → late case A/B mass transfer → BHG/WNLh + OB III-V → WNo + OB III-V → WC + OB III-V → SN + binary disruption → NS + OB I-III.
> *Single channel*: O6-7 V → O8-9 III → O9-B3 Ia → B5-9 Ia^{+}/YHG → RSG → B5-9 Ia^{+}/YHG/LBV → WN → WC(/WO?) → SN (leading to BH formation?)

[5] Similar quantities of helium would also be transfered but would have a negligible effect on the abundances of Wd1-5

Comprising two distinct populations, the BHGs within Wd 1 provide an elegant illustration of this scheme. The first, consisting of the late B5-9 Ia^{+} stars Wd1-7, -33 and -42a, lack observational signatures of binarity and appear to originate via single star evolution as the stars evolve from the main sequence and execute a red loop across the HR diagram.

The second, made up of the hybrid early BHG/WNLh objects Wd1-5, -13 and -44, all show clear signatures of current or historic binarity (e.g. periodic RV variability and/or hard, overluminous X-ray emission; Clark et al. 2008; Ritchie et al. 2010; and in prep.). Indeed, their spectral similarity (Figs. 2–4) suggest they have all experienced binary driven mass loss. With an orbital period of ~9.13 days, Wd1-13 is likely to undergo late case A/case B mass transfer and with $M_{\rm init}$ ~ 41 $M_{\odot}$+ ~ 30 $M_{\odot}$ will not experience the reversal of SNe order we anticipate for our putative Wd1-5 binary (Ritchie et al. 2010).

Initial analysis of multi-epoch RV observations of Wd1-44 (Ritchie et al., in prep.) suggests a period of $\lesssim$9 d, which is potentially consistent with the case A mass transfer we propose for Wd1-5. Moreover, with a secondary of apparently earlier spectral type – and hence more massive – than the O supergiant companion in Wd1-13 (for which we find $M_{\rm current}$ ~ $35.4^{+5.0}_{-4.6}$ $M_{\odot}$) it may represent a precursor of our putative Wd1-5 binary prior to the common envelope phase (and subsequent brief episode of reverse mass transfer that distinguishes Wd1-5 from the other two stars via the resultant C-enrichment).

We also identify a larger population of massive compact, interacting OB+OB binaries within Wd1 (e.g. Wd1-30a, -36 and -53; Clark et al. 2008; Ritchie et al., in prep.) that provide a rich reservoir of progenitors from which systems such as Wd1-5, -13 and -44 may be drawn. In particular we highlight the binary supergiant B[e] star Wd1-9, which currently appears to be undergoing the rapid case A evolution we hypothesise for Wd1-5 (Fig. 10; Clark et al. 2013).

5. A physical connection between Wd1-5 and CXOU J1647-45?

Two mechanisms have been invoked to explain the runaway phenomenon; dynamical ejection from dense stellar systems; (Poveda et al. 1967) and SN kicks in binary systems (Blaauw 1961). *N*-body simulations of both Wd1 and the young massive cluster R136 demonstrate that dynamical ejection of massive stars with velocities ranging up to ~300 km s^{-1} is well underway by ~3 Myr (Banerjee et al. 2012; Fujii et al. 2012). Conversely, at the age of Wd 1 we would expect SNe every 7−13 000 yr (Muno et al. 2006a,b); trivially, the presence of the magnetar confirms the recent occurrence of a SN.

Both mechanisms therefore appear viable for the ejection of Wd1-5, although a key discriminator between dynamical and SN ejection mechanisms is that under the latter scenario mass transfer from the SN progenitor may result in anomalous physical properties of the runaway. Wd1-5 shows evidence of C-enrichment that can only be understood via binary interaction, *strongly favouring the SN kick model for the formation of Wd1-5*. Indeed, if Wd1-5 were ejected via dynamical interaction, it must still have followed an identical binary evolution to that described in Sect. 4 prior to this event, which would also have had to unbind the requisite evolved companion. Therefore, while such a sequence is in principle possible, it appears unnecessarily contrived in comparison to the SN scenario.

If the peculiar velocity imparted to Wd1-5 was the result of a SN kick, an obvious question is whether this was the event that

produced the magnetar J1647-45? Given the rarity of magnetars, a compelling case for cluster membership rather than chance superposition may be made for J1647-45 (Muno et al. 2006a). Moreover, spectral modelling of J1647-45 shows that the column density towards it is consistent both with that inferred for Wd1 (determined from optical reddening), as well as the column density towards other X-ray bright cluster members (Clark et al. 2008). Following these lines of argument, we adopt the hypothesis that it is a cluster member for the remainder of this study.

Therefore, if J1647-45 resides within Wd1, one would expect the putative pre-SN companion to also remain within the cluster; indeed if such an object were *not* present, the hypothesis that binary driven mass loss permitted the formation of a NS rather than a BH would be seriously challenged. Are the physical properties of Wd1-5 – e.g. composition, luminosity, temperature, surface gravity and velocity relative to J1647-45 – consistent with such an hypothesis?

The displacement between J1645-47 and Wd1-5 of ∼139″ implies a minimum separation of ∼3.4 pc at a distance of 5 kpc. Assuming a characteristic age of the order of 10^4 yr for magnetars (e.g. Kouveliotou et al. 1994; Woods et al. 2006) leads to a relative projected velocity between the two objects of ∼325 km s^{-1}. To date direct measurements of the *transverse* velocities of six magnetars have been made, all of which are encouragingly modest (≤350 km s^{-1})[6] and hence consistent with the above estimate for the J1645-47/Wd1-5 system. Moreover, the association of three anomalous X-ray pulsars with supernovae remnants further supports the adoption of rather low magnetar kick velocities (despite theoretical predictions to the contrary; Mereghetti 2008). For comparison, a mean velocity of ∼400 km s^{-1} has been reported for young (<3 Myr) pulsars, with a maximum velocity of ∼1600 km s^{-1} (Hobbs et al. 2005). Given these findings, the separation of both Wd1-5 and J1645-47 appears consistent with a common origin.

Moreover, as highlighted in Sect. 3.2, the anomalous C-abundance of Wd1-5 (C/C$_\odot$ ∼ 1.4) is also present in the B1 Ia$^+$ and O6.5 Iaf$^+$ hypergiant mass donors in the X-ray binaries GX301-2 and 4U1700-37. As with our putative Wd1-5 + J1647-45 binary, the current physical properties of both binaries imply pre-SN mass transfer onto the current mass donor (Wellstein & Langer 1999; Clark et al. 2002; Kaper et al. 2006). Additionally, the lifetime of the C-abundance anomaly is expected to be rather short. Critically, acting on the *thermal* timescale (e.g. Wellstein et al. 2001; Petrovic et al. 2005), thermohaline, rather than rotational, mixing is expected to act to rapidly dilute the carbon overabundance resulting from the pre-SN mass transfer. So one would expect that dilution would already be well advanced after only 10^4 yr; a timescale directly comparable to the lifetime inferred for magnetars. Indeed, the similarity in the timescale for carbon dilution to the lifetime of a magnetar implies that the cessation of mass transfer to Wd1-5 and the event that formed J1647-45 must have occurred quasi-simultaneously.

We can also advance three additional arguments to bolster this association. No other magnetar or young cooling neutron star candidate that could have formed the requisite companion to Wd1-5 has been identified in either the original dataset or subsequent multi-epoch X-ray observations (Muno et al. 2006a; Clark et al. 2008; Woods et al. 2011). Conversely, despite extensive optical and near-IR surveys (Negueruela et al. 2010; Crowther et al. 2006a), no other plausible pre-SN binary companion to J1647-45 has been identified within the massive stellar population of Wd1. Moreover, given the preceding estimate of the mean interval between consecutive SNe within Wd1 at this epoch, one would expect the observed runaway velocity of Wd1-5 to carry it beyond the cluster confines before the next such event – i.e. if the velocity of Wd1-5 is representative of that imparted to runaway stars at SN, on average one would expect only one such object to be present within Wd1 at this time – and hence on statistical grounds we would expect both magnetar and Wd1-5 to be physically associated with one another.

So in summary, all the available evidence points to the anomalous RV of Wd1-5 as being the result of a SNe kick. In particular, the carbon abundance points to a recent episode of mass transfer from a close companion, although *currently* there is no observational evidence of such an object. Moreover, the timescale for dilution of the abundance anomalies is comparable to the duration of the magnetar phase, while the angular separation of both Wd1-5 and J1647-45 is also consistent with known magnetar and pulsar kick velocities. Therefore, while the absence of transverse velocity measurements prevents a definitive association, we can identify strong lines of argument to posit a physical association between Wd1-5 and J1647-45 in a pre-SN binary system.

6. Implications for magnetar formation

If the hypothesis that Wd1-5 and the magnetar J1647-45 comprised a pre-SN binary system is correct, what are the physical implications? No consensus yet exists on the formation mechanism for magnetars. Gaensler et al. (2005) suggested their progenitors were limited to particularly massive stars (≳40 $M_\odot$); however, more recent observations suggest that they instead span a wide range of masses (∼17−50 $M_\odot$; Sect. 1), implying that additional physical factors must drive this process.

Duncan & Thompson (1992) and Thompson & Duncan (1993) argued for their formation via rapidly rotating (P ∼ 1 ms) proto-NSs, when a large-scale convective dynamo may generate an extreme magnetic field in the first few seconds after birth. However, if magnetic torques are successful at removing angular momentum from the core via coupling to the extended atmosphere present in a pre-SN RSG phase, then the core will not be rotating rapidly enough at SN for this mechanism to operate (e.g. Heger et al. 2005). Moreover such a scenario would predict both highly energetic SNe and high spatial velocities for the resultant magnetars (e.g. Duncan & Thompson 1992) which appear to be in conflict with observations (e.g. Mereghetti 2008; Vink & Kuiper 2006). An alternative suggestion is the "fossil field" hypothesis, whereby a pre-existing magenetic field acquired at the birth of the progenitor is amplified during stellar collapse. Spruit (2008) argued against this mechanism given the lack of sufficient numbers of highly magnetised stars to explain the expected formation rate of magnetars and, once again, the fact that core-envelope coupling will result in spin down of the core.

How does J1647-45 inform the debate? The Wd1 RSGs cohort implies that *if* the progenitor of J1647-45 had been a single star, it would have passed through such a phase and hence have been subject to spin-down via core-envelope coupling. While we cannot exclude an unusually strong (fossil) magnetic field in the progenitor of J1647-45, we find no evidence of a corresponding

[6] $v = 212 \pm 35(d/3.5\ \mathrm{kpc})$ km s^{-1} for XTE J1810-197 (Helfand et al. 2007), $v = 280^{+130}_{-120}$ km s^{-1} for PSR J1550-5418 (Deller et al. 2012), $v = 350 \pm 100(d/9\ \mathrm{kpc})$ km s^{-1} for SGR 1806-20 and $v = 130 \pm 30(d/12.5\ \mathrm{kpc})$ km s^{-1} for SGR 1900+14 (both Tendulkar et al. 2012) and $v = 157 \pm 17$ km s^{-1} for AXP 1E 2259+586 and $v = 102 \pm 26$ km s^{-1} for AXP 4U 0142+61 (both Tendulkar et al. 2013).

population of highly magnetic massive stars within Wd1 at this time[7].

Binarity has been invoked under both scenarios as an additional ingredient in order to avoid core-envelope coupling, by removing the outer layers of the SN progenitor and thus preventing a RSG phase, so that sufficient angular momentum is retained in the core to form a magnetar[8]. Moreover, the high mass implied for the progenitors of both J1647-45 and SGR1806-20 (Sect. 1) suggests that binary driven mass loss resulting in the early onset of WR mass loss rates and hence the production of a low-mass pre-SN core was likewise essential to the formation of a magnetar rather than a BH (cf. Fryer et al. 2002).

An additional point of interest is whether the pre-SN evolution of a massive compact binary system – such as we infer for J1647-45 – favours the production of a seed magnetic field, which is subsequently amplified during or shortly after core collapse to yield a magnetar (e.g. Spruit 2008). Following Langer (2012), both mass transfer and stellar merger in compact binaries may lead to dramatic spin-up of the mass-gainer/merger remnant, potentially favouring the formation of a magnetic field via dynamo action. In support of such an hypothesis we highlight the detection of a magnetic field in the rapidly rotating secondary in Plaskett's star (Grunhut et al. 2013); a higher mass analogue of our putative Wd1-5+J1647-45 binary, which has also undergone case A mass transfer (e.g. Linder et al. 2008).

Alternatively, Tout et al. (2008) suggested that high magnetic field white dwarfs may form via strong binary interactions between a main sequence and red giant (and hence white-dwarf progenitor) in a common envelope phase. In this scenario as the orbital period of the 2 components decreases, differential rotation within the convective common envelope generates the magnetic field via dynamo action; one might speculate that a comparable process also occurs in high mass analogues, such as the pre-SN LBV/common envelope phase we propose here (Sect. 4.1).

A binary mediated formation scenario would suppose that if merger is avoided[9] one could anticipate identifying the pre-SN magnetar companion. The proper motion study of Tendulkar et al. (2012; footnote 6) places the birthsite of SGR1806-20 within the confines of the eponymous host cluster, with the positional uncertainty elipse encompassing three stars. Of these, object D has been classified as an OB supergiant, and hence potentially the massive pre-SN companion we predict; classification spectroscopy of the remaining stars in combination with an RV survey of the full cluster population would be of considerable interest to determine if any of the three are indeed overluminous chemically peculiar runaway analogues to Wd1-5. Alternatively, if disruption is avoided, binaries containing magnetars should also exist. In this regard the suggestion of Reig et al. (2012) that the neutron star within the X-ray binary 4U2206+54 is a magnetar is of considerable interest, moreso given that the combination of short ($P_{\rm orb}$ ~ 10 day) period and He-rich nature of the primary is suggestive of pre-SN binary interaction in the system.

Potential observational biases in the detection of quiescent magnetars hamper a *direct* determination of their birth rate, although several authors have suggested it may be comparable to that of radio pulsars (e.g. Muno et al. 2008; Woods 2008); confirmation of a binary channel for magnetar formation would allow us to address this issue. Intriguingly, recent observations suggest a high (≥40%; e.g. Sana et al. 2012; Kiminki & Kobulnicky 2012; Chini et al. 2012; Ritchie et al., in prep.) binary fraction amongst OB stars, an orbital period distribution favouring short-period systems with respect to the classical Öpik's Law (a flat distribution of orbital separations in logarithmic space) and a mass ratio favouring more massive companions (i.e. inconsistent with random selection from a Kroupa type initial mass function); all factors potentially favouring the production of magnetars under the above scenario. Indeed, the presence of a number of compact OB+OB binaries and a massive binary fraction of >70% amongst the WR population (Clark et al. 2008) potentially provides a rich progenitor reservoir within Wd1, with Wd1-44 being the most compelling example currently identified (Sect. 4.2).

7. Concluding remarks

The presence of a magnetar with a progenitor mass ≳40 $M_\odot$ within Wd 1 requires a mechanism by which significant mass loss can occur prior to SN, with binary interaction a leading candidate. Therefore, the identification of a pre-SN companion to J1647-45 provides a critical test of the theory. As part of our RV survey of the cluster we identified the single star Wd1-5 as a runaway – and hence a potential candidate.

To date no other massive star – either within Wd1 or part of the wider Galactic population – completely reproduces the spectral morphology and/or combination of physical properties of Wd1-5. Quantitative analysis reveals physical properties inconsistent with the evolution of a single star (Sect. 3). In particular the anomalously high C-abundance of Wd1-5 in comparison to the predicted CNO abundances is inexplicable under such a scenario and has previously only been observed in the mass donors of the X-ray binaries GX301-2 and 4U1700-37. In both cases this is thought to result from a brief episode of wind driven mass transfer from a C-rich WC Wolf-Rayet binary companion which, post-SN, formed the relativistic companion.

Motivated by these findings, we used the combination of spectroscopic mass, luminosity and chemical abundances of Wd1-5 to infer a pre-SN evolutionary history for the putative binary (Sect. 4). Significant case A mass transfer from Wd1-5 leads to spin-up of the companion, which consequently evolves more rapidly than the mass donor, resulting in a subsequent LBV-driven common-envelope phase which strips its H-rich mantle. The initially less massive companion then enters the WR phase, triggering an enrichment of the atmosphere of Wd1-5 by the stellar wind of the by then WC star, which then explodes as a type Ibc SN, unbinding the binary. In support of this hypothesis we highlight that the observational properties of the remaining early-BHG/WNLhs within Wd1 – Wd1-13 and -44 – reveal them both to be short-period interacting binaries, while a large reservoir of progenitor binaries has also been identified (Ritchie et al., in prep.).

Given this, a natural explanation for the runaway nature for Wd1-5 is that it was ejected via a SN kick and we present a

[7] By analogy to the optical properties of Of?p stars, Clark et al. (2010) cited Wd1-24 as a possible highly magnetic star, based on the variable C III+Pa 16 ~8500 Å blend. However, further observations have revealed that this behaviour is instead due to a variable contribution from a late-O binary companion (Ritchie et al., in prep.). Known magnetic OB stars are expected to demonstrate hard, overluminous X-ray emission (e.g. Clark et al. 2009a, and refences therein); while several overluminous OB stars are present within Wd 1 (Clark et al. 2008), they all demonstrate rather soft X-ray spectra; the sole exception being W30a, a known (colliding wind) binary.

[8] Although simulations by Yoon et al. (2010) suggests that such a mechanism is ineffective for stars below 25 $M_\odot$.

[9] Under such a scenario we might suppose the lack of a luminous stellar source associated with the wind blown bubble hosting the magentar 1E 1048.1-5937 (Gaensler et al. 2005) would be explicable if the binary merged prior to SN.

number of lines of argument to support a physical association with the magnetar J1647-45 (noting that the conclusions above are *not* dependant on such a connection). Under this hypothesis, binarity plays a critical role in the formation of the magnetar by (i) preventing the spin-down which happens in single stars via core-envelope coupling because the envelope is removed and (ii) enabling the formation of a low-mass pre-SN core via the prolonged action of WR-phase winds. Moreover, we may speculate that the binary interaction results in the generation of a seed magnetic field in the magnetar progenitor via dynamo action, either during the spin up of the mass gainer or in a subsequent LBV/common envelope phase.

If correct, while the BHG/WNLh stars Wd1-5, -13 and -44 might be expected to form a NS rather than a BH as a result of their binary driven mass loss, they have not been spun up by mass transfer and therefore do not replicate the properties of our putative magnetar progenitor. While the secondary in Wd-13 has been spun up via mass transfer, it remains insufficiently massive for the SN order to be reversed, as we propose for Wd1-5, and consequently will follow a different evolutionary path whereby magnetic core-envelope coupling is not avoided. However, the secondary in Wd1-44 appears more massive and we might suppose this system will follow a similar pathway to Wd1-5, and hence potentially yield a magnetar.

As well as permitting a determination of the magnetar formation rate via the identification of the binary progenitor population, the presence of carbon pollution in the atmosphere of Wd1-5 supposes an H-depleted WC Wolf-Rayet as the immediate magnetar progenitor, which would have exploded as a type Ibc SN. This would be the first association of the birth of a magnetar with such an event and would also support the assertion that massive close binary evolution is a promising channel for the production of a subset of type Ibc SNe. Indeed current observational studies suggest that binary stripping is important in the production of the majority of type Ibc SNe, albeit from a population of lower mass ($\leq$20−25 $M_{\odot}$) progenitors than we assume here (Smith et al. 2011; Eldridge et al. 2013; Kuncarayakti et al. 2013).

Expanding upon this and a number of authors have suggested that magnetars may power superluminous type II and Ibc SNe (Thompson et al. 2004; Woosley 2010; Kasen & Bildsten 2010; Gal-Yam 2012; Quimby et al. 2011); indeed the 7.29 $M_{\odot}$ progenitor model of Woosley (2010) is directly motivated by the presence of J1647-45 within Wd1. Moreover, Inserra et al. (2013) studied the late-time lightcurves of five superluminous type Ic SNe, finding that the data are indeed consistent with these events being powered by the rapid spin-down of newly born magnetars (see also McCrum et al. 2013; Nicholl et al. 2013) Additionally, magnetars have also been proposed as the central engines of some gamma-ray bursts (GRBs; e.g. Usov 1992; Duncan & Thompson 1992; Metzger et al. 2011, and refs. therein). Given the latter suggestion it is therefore intriguing that long duration GRBs have been associated with type Ibc SNe (e.g. Della Valle 2006).

If such an hypothesis is viable, one might ask why such superluminous events are not more common in the local Universe if the magnetar formation rate is indeed a substantial percentage of that of neutron stars (e.g. Muno et al. 2008)? One plausible explanation may be that the superluminous SNe occur in low metallicity environments where correspondingly weak stellar winds minimise pre-SNe angular momentum losses, leading to systematically more rapidly rotating magnetars and hence a greater deposition of energy in the SNe in comparison to the higher metallicity local environment. In any event, given the apparent ubiquity of massive compact binaries, additional theoretical and observational investigations of the potential link between binary mediated formation channels for magnetars, (superluminous) type Ibc SNe and GRBs would clearly be of considerable interest.

Acknowledgements. This research is partially supported by the Spanish Ministerio de Ciencia e Innovación (MICINN) under grant AYA2012-39364-C02-02.

References

Anders, E., & Grevesse, N. 1989, GeCoA, 53, 197
Appenzeller, I., Fricke, K., Fürtig, W., et al. 1998, The Messenger, 94, 1
Asplund, M., Grevesse, N., & Jacques Sauval, A. 2006, Nucl. Phys. A, 777, 1
Banerjee, S., Kroupa, P., & Oh, S. 2012, ApJ, 746, 15
Bibby, J. L., Crowther, P. A., Furness, J. P., & Clark, J. S. 2008, MNRAS, 386, L23
Blaauw, A. 1961, Bull. Astron. Inst. Netherlands, 15, 265
Bohannan, B., & Crowther, P. A. 1999, ApJ, 511, 374
Bonanos, A. Z. 2007, AJ, 133, 2696
Braun, H., & Langer, N. 1995, A&A, 297, 483
Brott, I., de Mink, S. E., Cantiello, M., et al. 2011, A&A, 530, A115
Brown, G. E., Heger, A., Langer, N., et al. 2001, New Astron., 6, 457
Cardelli, J. A., Clayton, G. C., & Mathis, J. S. 1989, ApJ, 345, 245
Chini, R., Hoffmeister, V. H., Nasseri, A., Stahl, O., & Zinnecker, H. 2012, MNRAS, 424, 1925
Clark, J. S., Goodwin, S. P., Crowther, P. A., et al. 2002, A&A, 392, 909
Clark, J. S., Negueruela, I., Crowther, P. A., & Goodwin, S. P. 2005, A&A, 434, 949
Clark, J. S., Muno, M. P., Negueruela, I., et al. 2008, A&A, 347, 147
Clark, J. S., Davies, B., Najarro, F., et al. 2009a, A&A, 504, 429
Clark, J. S., Crowther, P. A., Larionov, V. M., et al. 2009b, A&A, 507, 1555
Clark, J. S., Ritchie, B. W., & Negueruela, I. 2010, A&A, 514, A87
Clark, J. S., Ritchie, B. W., Negueruela, I., et al. 2011, A&A, 531, A28
Clark, J. S., Najarro, F., Negueruela, I., et al. 2012, A&A, 541, A145
Clark, J. S., Ritchie, B. W., & Negueruela, I. 2013, A&A, 560, A11
Cottaar, M., Meyer, M., Andersen, M., & Espinoza, P. 2012, A&A, 539, A5
Crowther, P. A., Hadfield, L. J., Clark, J. S., Negueruela, I., & Vacca, W. D. 2006a, MNRAS, 372, 1407
Crowther, P. A., Lennon, D. J., & Walborn, N. R. 2006b, A&A, 446, 279
Cruz-González, C., Recillas-Cuz, E., Costero, R., Peimbert, M., & Torres-Peimbert, S. 1974, Rev. Mex. Astron. Astrofis., 1, 211
Davies, B., Figer, D. F., Kudritzki, R.-P., et al. 2009, ApJ, 707, 844
Della Valle, M. 2006, in Gamma Ray Burts in the Swift Era, Washington, D. C., eds. S. Holt, N. Gehrels, & J. A. Nousek, AIP, 836, 367
Deller, A. T., Camilo, F., Reynolds, J. E., & Halpern, J. P. 2012, ApJ, 748, L1
Dessart, L., Langer, N., & Petrovic, J. 2003, A&A, 404, 991
Dougherty, S. M., Clark, J. S., Negueruela, I., Johnson, T., & Chapman, J. M. 2010, A&A, 511, A58
Duncan, R. C., & Thompson, C. 1992, ApJ, 392, L9
Ekström, S., Georgy, C., Eggenberger, P., et al. 2012, A&A, 537, A146
Eldridge, J. J., Fraser, M., Smartt, S. J., Maund, J. R., & Crockett, R. M. 2013, MNRAS, 436, 774
Figer, D. F., Najarro, F., Geballe, T. R., Blum R. D., & Kudritzki, R. P. 2005, ApJ, 622, L49
Fryer, C. L., Heger, A., Langer, N., & Wellstein, S. 2002, ApJ, 578, 335
Fujii, M. S., Saitoh, T. R., & Portegies Zwart, S. F. 2012, ApJ, 753, 85
Fullerton, A. W., Massa, D. L., & Prinja, R. K. 2006, ApJ, 637, 1025
Gaensler, B. M., McClure-Griffiths, N. M., Oey, M. S., et al. 2005, ApJ, 620, L95
Gal-Yam, A. 2012, Science, 337, 927
Gräfener, G., Vink, J. S., de Koter & A., Langer, N. 2011, A&A, 535, A56
Groh, J. H., Hillier, D. J., Damineli, A., et al. 2009a, ApJ, 698, 1698
Groh, J. H., Hillier, D. J., Damineli, A., et al. 2009b, ApJ, 705, L25
Grunhut, J. H., Wade, G. A., Leutenegger, M., et al. 2013, MNRAS, 428, 1686
Heger, A., Woosley, S. E., & Spruit, H. C. 2005, ApJ, 626, 350
Helfand, D. J., Chatterjee, S., Brisken, W. F., et al. 2007, ApJ, 662, 1198
Hillier, D. J., & Miller, D. L. 1998, ApJ, 496, 407
Hillier, D. J., & Miller, D. L. 1999, ApJ, 519, 354
Hillier, D. J., Crowther, P. A., Najarro, F., & Fullerton, A. W. 1998, A&A, 340, 483
Hillier, D. J., Davidson, K., Ishibashi, K., & Gull, T. 2001, ApJ, 553, 837
Hobbs, G., Lorimer, D. R., Lyne, A. G., & Kramer, M. 2005, MNRAS, 360, 974
Inserra, C., Smartt, S. J., Jerkstrand, A., et al. 2013, ApJ, 770, 128
Kaper, L., van der Mer, A., & Najarro, F. 2006, A&A, 457, 595

Kasen, D., & Bildsten, L. 2010, ApJ, 717, 245
Kiminki, D. C., & Kobulnicky, H. A. 2012, ApJ, 751, 4
Kothes, R., & Dougherty, S. M. 2007, A&A, 468, 993
Koumpia, E., & Bonanos, A. Z. 2012, A&A, 547, A30
Kouveliotou, C., Fishman, G. J., Meegan, C. A., et al. 1994, Nature, 368, 125
Kudryavtseva, N., Brandner, W., Gennaro, M., et al. 2012, ApJ, 750, L44
Kuncarayakti, H., Doi, M., Aldering, G., et al. 2013, AJ, 146, 30
Laming, J. M. & Hwang, U. 2003, ApJ, 597, 347
Langer, N. 1998a, A&A, 210, 93
Langer, N. 1998b, A&A, 329, 551
Langer, N. 2012, ARA&A, 50, 107
Lefever, K., Puls, J., & Aerts, C. 2007, A&A, 463, 1093
Linder, N., Rauw, G., Martins, F., et al. 2008, A&A, 489, 713
Luna, A., Mayya, Y. D., Carrasco, L., Rodríguez-Merino, L. H., & Bronfman, L. 2009, Rev. Mex. Astron. Astrofis., 37, 32
Maeder, A., & Meynet, G. 2000, A&A, 361, 159
Markova, N., & Puls, J. 2008, A&A, 478, 822
Martins, F., Genzel, R., Hillier, D. J., et al. 2007, A&A, 468, 233
Mason, A. B., Clark, J. S., Norton, A. J., et al. 2012, A&A, 422, A199
McCrum, M., Smartt, S. J., Kotak, R. et al. 2013, MNRAS, 437, 656
Mengel, S., & Tacconi-Garman, L. E. 2009, ApSS, 324, 321
Mereghetti, S. 2008, A&ARv, 15, 225
Metzger, B. D., Giannios, D., Thompson, T. A., Bucciantini, N., & Quataert, E. 2011, MNRAS, 413, 2031
Meynet, G., & Maeder, A. 2000, A&A, 361, 101
Mokiem, M. R., de Koter, A., Vink, J. S., et al. 2007, A&A, 473, 603
Mori, K., Gotthelf, E. V., Zhang, S., et al. 2013, ApJ, 770, L23
Muno, M. P. 2007, AIPC, 924, 166
Muno, M. P., Clark, J. S., Crowther, P. A., et al. 2006a, ApJ, 636, L41
Muno, M. P., Law, C., Clark, J. S., et al. 2006b, ApJ, 650, 203
Muno, M. P., Gaensler, B. M., Nechita, A., Miller, J. M., & Slane, P. O. 2008, ApJ, 680, 639
Najarro, F. 2001, P Cygni 2000: 400 years of Progress, eds. M. de Groot, & C. Sterken (San Francisco, CA:ASP), ASP Conf. Ser., 233, 133
Najarro, F., Hillier, D. J., & Stahl, O. 1997, A&A, 326, 1117
Najarro, F., Hillier, D. J., Puls, J., Lanz, T., & Martins, F. 2006, A&A, 456, 659
Najarro, F., Figer, D. F., Hillier, D. J., Geballe, T. R., & Kudritzki, R. P. 2009, ApJ, 691, 1816
Negueruela, I., Clark, J. S., & Ritchie, B. W. 2010, A&A, 516, A78
Nicholl, M., Smartt, S. J., & Jerkstrand, A. 2013, Nature, 503, 236
Nomoto, K., Sugmioto, D., Sparks, W. M., et al. 1982, Nature, 299, 803
Pasquini, L., Avila, G., Blecha, A., et al. 2002, The Messenger, 110, 1
Petrovic, J., Langer, N., & van der Hucht, K. A. 2005, A&A, 435, 1013
Poveda, A., Ruiz, J., & Allen, C. 1967, Bol. Obs. Tonantzintla y Tacubaya, 4, 86
Quimby, R. M., Kulkarni, S. R., Kasliwal, M. M., et al. 2011, Nature, 474, 487
Reig, P., Torjón, J. M., & Blay, P. 2012, MNRAS, 401, 595
Ritchie, B. W., Clark, J. S., Negueruela, I., & Crowther, P. A. 2009a, A&A, 507, 1585
Ritchie, B. W., Clark, J. S., Negueruela, I., & Najarro, F. 2009b, A&A, 507, 1597
Ritchie, B. W., Clark, J. S., Negueruela, I., & Langer, N. 2010, A&A, 520, A48
Sana, H., de Mink, S. E., de Koter, A., et al. 2012, Science, 337, 444
Searle, S. C., Prinja, R. K., Massa, D., & Ryans, R. 2008, A&A, 481, 777
Smith, N. Li,W., Filippenko, A. V., & Chornock, R. 2011, MNRAS, 412, 1522
Spruit, H. C. 2008, in 40 years of pulsars:millisecond pulsars, magnetars and more, AIP Conf. Proc., 983, 391
Tendulkar, S. P., Cameron, P. B., & Kulkarni, S. R. 2012, ApJ, 761, 761
Tendulkar, S. P., Cameron, P. B., & Kulkarni, S. R. 2013, ApJ, 772, 31
Tetzlaff, N., Neuhäuser, R., & Hohle, M. M. 2011, MNRAS, 410, 190
Thompson, C., & Duncan, R. C. 1993, ApJ, 408, 194
Thompson, T. A., Chang, P., & Quataert, E. 2004, ApJ, 611, 380
Tout, C. A., Wickramasinghe, D. T., Liebert, J., Ferrario, L., & Pringle, J. E. 2008, MNRAS, 387, 897
Usov, V. V. 1992, Nature, 357, 472
Vink, J., & Kuiper, L. 2006, MNRAS, 370, L14
Vink, J. S., de Koter, A., & Lamers, H. J. G. L. M. 2000, A&A, 362, 295
Vitrichenko, E. A., Gershberg, R. E., & Metik, L. P. 1965, IzKry, 34, 193
Wellstein, S., & Langer, N. 1999, A&A, 350, 148
Wellstein, S., Langer, N., & Braun, H. 2001, A&A, 369, 939
Woods, P. M. 2008, in 40 years of pulsars:millisecond pulsars, magnetars and more, AIP Conf. Proc., 983, 227
Woods, P. M., & Thompson, C. 2006 in Compact stellar X-ray sources, eds. W. Lewin, & M. van der Klis (Cambridge University Press), Cambridge Astrophys. Ser., 39, 547
Woods, P. M., Kaspi, V. M., Gavriil, F. P., & Airhart, C. 2011, ApJ, 726, 37
Woosley, S. E. 2010, ApJ, 719, L204
Yoon, S.-C., Woosley, S. E., & Langer, N. 2010, ApJ, 725, 940
Young, P. A., Fryer, C. L., Hungerford, A., et al. 2006, ApJ, 640, 891

Appendix A: Summary of stellar comparison data to Wd1-5

Table A.1. Comparison of basic stellar parameters of Wd1-5 to those of related galactic stars.

Name	Spec. Type	$\log(L_*)$ ($L_\odot$)	R_* ($R_\odot$)	$T_{\rm eff}$ (kK)	$\log g$	$\log(\dot{M})$ ($M_\odot$ yr^{-1})	v_∞ (km s^{-1})	Reference
Wd1-5	B0.5 Ia$^+$	$5.38^{+0.12}_{-0.12}$	$34.0^{+5.0}_{-4.4}$	$21.05^{+1.5}_{-1.2}$	$2.33^{+0.17}_{-0.10}$	$-5.36^{+0.3}_{-0.2}$	430^{+20}_{-40}	This work
HD 30614	O9.5 Ia	5.63	26.0	29.0 ± 1.0	3.0 ± 0.15	$-5.30^{+0.11}_{-0.15}$	1560	1
HD 168183	O9.5 Ib	5.42 ± 0.22	$19.0^{+4.3}_{-3.5}$	30.0 ± 1.0	3.3 ± 0.1	$-6.82^{+0.24}_{-0.24}$	1700 ± 510	2
HD 37128	B0 Ia	5.44	24.0	27.0 ± 1.0	2.9 ± 0.15	$-5.60^{+0.11}_{-0.15}$	1910	1
HD 89767	B0 Ia	5.35 ± 0.22	$30.0^{+6.7}_{-5.5}$	23.0 ± 1.0	2.55 ± 0.1	$-6.07^{+0.24}_{-0.24}$	1600 ± 480	2
HD 91969	B0 Ia	5.52	25.3	27.5 ± 1.0	2.75 ± 0.14	$-6.00^{+0.11}_{-0.15}$	1470	1
HD 94909	B0 Ia	5.49	25.5	27.0 ± 1.0	2.9 ± 0.14	$-5.70^{+0.11}_{-0.15}$	1050	1
HD 122879	B0 Ia	5.52	24.4	28.0 ± 1.0	2.95 ± 0.14	$-5.52^{+0.11}_{-0.15}$	1620	1
HD 192660	B0 Ib	5.74 ± 0.13	23.4 ± 1.0	30.0 ± 1.0	3.25	$-5.30^{+0.00}_{-0.40}$	1850	3
HD 204172	B0.2 Ia	5.48 ± 0.27	22.4 ± 3.2	28.5 ± 1.0	3.13	$-6.24^{+0.34}_{-0.40}$	1685	3
HD 38771	B0.5 Ia	5.35	22.2	26.5 ± 1.0	2.9 ± 0.14	$-6.05^{+0.11}_{-0.15}$	1525	1
HD 115842	B0.5 Ia	5.65	34.2	25.5 ± 1.0	2.85 ± 0.14	$-5.70^{+0.11}_{-0.15}$	1180	1
HD 152234	B0.5 Ia	5.87	42.4	26.0 ± 1.0	2.85 ± 0.14	$-5.57^{+0.11}_{-0.15}$	1450	1
HD 185859	B0.5 Ia	5.54 ± 0.14	29.1 ± 1.3	26.0 ± 1.0	3.13	$-6.30^{+0.08}_{-0.10}$	1830	3
HD 64760	B0.5 Ib	5.48 ± 0.26	23.3 ± 2.2	28.0 ± 2.0	3.38	$-5.96^{+0.28}_{-1.04}$	1600	3
HD 93619	B0.5 Ib	5.30 ± 0.22	$22.0^{+4.9}_{-4.1}$	26.0 ± 1.0	2.9 ± 0.1	$-6.12^{+0.24}_{-0.24}$	1470 ± 441	2
HD 213087	B0.5 Ib	5.69 ± 0.11	32.0 ± 0.01	27.0 ± 1.0	3.13	$-6.15^{+0.19}_{-0.0}$	1520	3
HD 2905	BC0.7 Ia	5.52	41.4	21.5 ± 1.0	2.6 ± 0.14	$-5.70^{+0.11}_{-0.15}$	1105	1
HD 91943	B0.7 Ia	5.35	26.3	24.5 ± 1.0	2.8 ± 0.14	$-6.12^{+0.11}_{-0.15}$	1470	1
HD 152235	B0.7 Ia	5.76	47.1	23.0 ± 1.0	2.65 ± 0.14	$-5.90^{+0.11}_{-0.15}$	850	1
HD 154090	B0.7 Ia	5.48	36.0	22.5 ± 1.0	2.65 ± 0.14	$-6.02^{+0.11}_{-0.15}$	915	1
HD 96880	B1 Ia	5.42 ± 0.11	$43.0^{+9.7}_{-7.9}$	20.0 ± 1.0	2.4 ± 0.1	$-6.40^{+0.24}_{-0.24}$	1200 ± 360	2
HD 115363	B1 Ia	5.42 ± 0.11	$43.0^{+9.7}_{-7.9}$	20.0 ± 1.0	2.4 ± 0.1	$-5.92^{+0.24}_{-0.24}$	1200 ± 360	2
HD 148688	B1 Ia	5.45	36.7	22.0 ± 1.0	2.60 ± 0.14	$-5.76^{+0.11}_{-0.15}$	725	1
HD 170938	B1 Ia	5.42 ± 0.11	$43.0^{+9.7}_{-7.9}$	20.0 ± 1.0	2.4 ± 0.1	$-6.15^{+0.24}_{-0.24}$	1200 ± 360	2
HD 13854	B1 Iab	5.43	37.4	21.5 ± 1.0	2.55 ± 0.14	$-6.07^{+0.11}_{-0.15}$	920	1
HD 91316	B1 Iab	5.47	37.4	22.0 ± 1.0	2.55 ± 0.14	$-6.46^{+0.11}_{-0.15}$	1110	1
HD 109867	B1 Iab	5.56 ± 0.22	$38.0^{+8.5}_{-7.0}$	23.0 ± 1.0	2.6 ± 0.1	$-6.30^{+0.24}_{-0.24}$	1400 ± 420	2
HD 190066	B1 Iab	5.54 ± 0.20	41.4 ± 1.9	21.0 ± 1.0	2.88	$-6.15^{+0.05}_{-0.07}$	1275	3
HD 47240	B1 Ib	4.93 ± 0.22	$27.0^{+6.1}_{-5.0}$	19.0 ± 1.0	2.4 ± 0.1	$-6.77^{+0.24}_{-0.24}$	1000 ± 300	2
HD 154043	B1 Ib	4.98 ± 0.22	$26.0^{+5.8}_{-5.3}$	20.0 ± 1.0	2.5 ± 0.1	$-6.70^{+0.24}_{-0.24}$	1300 ± 390	2
HD 54764	B1 Ib/II	4.90 ± 0.22	$26.0^{+5.8}_{-5.3}$	19.0 ± 1.0	2.45 ± 0.10	$-7.52^{+0.24}_{-0.24}$	900 ± 270	2
HD 14956	B1.5 Ia	5.65	50.6	21.0 ± 1.0	2.5 ± 0.14	$-6.00^{+0.11}_{-0.15}$	500	1
HD 106343	B1.5 Ia	5.40 ± 0.22	$42.0^{+9.4}_{-7.7}$	20.0 ± 1.0	2.50 ± 0.1	$-6.28^{+0.24}_{-0.24}$	800 ± 240	2
HD 193183	B1.5 Ib	5.00 ± 0.26	30.8 ± 2.8	18.5 ± 1.0	2.63	$-6.64^{+0.40}_{-0.00}$	565	3
HD 111990	B1/2 Ib	4.91 ± 0.22	$25.0^{+5.6}_{-4.5}$	19.5 ± 1.0	2.55 ± 0.10	$-6.85^{+0.24}_{-0.24}$	750 ± 225	2
HD 14143	B2 Ia	5.42	52.9	18.0 ± 1.0	2.25 ± 0.14	$-5.98^{+0.11}_{-0.15}$	645	1
HD 14818	B2 Ia	5.35	46.1	18.5 ± 1.0	2.4 ± 0.14	$-6.26^{+0.11}_{-0.15}$	565	1
HD 41117	B2 Ia	5.65	61.9	19.0 ± 1.0	2.35 ± 0.14	$-6.05^{+0.11}_{-0.15}$	510	1
HD 194279	B2 Ia	5.37	44.7	19.0 ± 1.0	2.3 ± 0.14	$-5.98^{+0.11}_{-0.15}$	550	1
HD 206165	B2 Ib	5.18 ± 0.26	39.8 ± 5.5	18.0 ± 0.5	2.50	$-6.30^{+0.00}_{-0.22}$	640	3
HD 141318	B2 II	4.56 ± 0.11	16.0	20.0 ± 1.0	2.90 ± 0.1	$-7.52^{+0.24}_{-0.24}$	900 ± 270	2
HD 92964	B2.5 Iae	5.33 ± 0.11	48.0	18.0 ± 1.0	2.1 ± 0.1	$-6.55^{+0.24}_{-0.24}$	520 ± 156	2
HD 198478	B2.5 Ia	5.03	40.0	16.5 ± 1.0	2.15 ± 0.14	$-6.64^{+0.11}_{-0.15}$	470	1
HD 42087	B2.5 Ib	5.11 ± 0.24	36.6 ± 1.7	18.0 ± 1.0	2.50	$-6.70^{+0.00}_{-0.40}$	650	3

Notes. Stars are presented from early to late spectral types for BSGs and BHGs and from hottest to coolest for the LBVs and WNLh stars. The lack of suitable absorption profiles prevents a determination of the surface gravity of the LBVs and WNLh stars. Throughout the table we employ the clumping corrected mass loss rate ($\dot{M}/\sqrt{f}$) to allow direct comparison between individual stars; hence the difference between this table and Table 1 for Wd1-5. Unfortunately errors are not presented for all physical parameters of all individual stars by the studies used in the construction of this table. Values for both high and low temperature states of AG Car are provided.

References. (1) Crowther et al. (2006b); (2) Lefever et al. (2007); (3) Searle et al. (2008); (4) Markova & Puls (2008); (5) Kaper et al. (2006); (6) Clark et al. (2012); (7) Groh et al. (2009a); (8) Najarro (2001); (9) Groh et al. (2009b); (10) Najarro et al. (2009); (11) Clark et al. (2009b); (12) Bohannan & Crowther (1999); (13) Martins et al. (2007).

Table A.1. continued.

Name	Spec. Type	$\log(L_*)$ ($L_\odot$)	R_* ($R_\odot$)	$T_{\rm eff}$ (kK)	$\log g$	$\log(\dot{M})$ ($M_\odot$ yr^{-1})	v_∞ (km s^{-1})	Reference
HD 14134	B3 Ia	5.28	56.7	16.0 ± 1.0	2.05 ± 0.14	$-6.28^{+0.11}_{-0.15}$	465	1
HD 53138	B3 Ia	5.34	65.0	15.5 ± 1.0	2.05 ± 0.14	$-6.44^{+0.11}_{-0.15}$	865	1
HD 58350	B5 Ia	5.18 ± 0.17	57.3 ± 2.6	15.0 ± 0.5	2.13	$-6.15^{+0.15}_{-0.00}$	320	3
HD 102997	B5 Ia	5.25 ± 0.22	$55.0^{+12.4}_{-10.1}$	16.0 ± 1.0	2.00 ± 0.1	$-6.64^{+0.24}_{-0.24}$	325 ± 98	2
HD 108659	B5 Ib	4.60 ± 0.22	$26.0^{+5.8}_{-5.3}$	16.0 ± 1.0	2.30 ± 0.1	$-7.22^{+0.24}_{-0.24}$	470 ± 141	2
HD 164353	B5 Ib	4.30 ± 1.30	19.6 ± 8.1	15.5 ± 1.0	2.75	$-7.22^{+0.00}_{-0.30}$	450	3
HD 80558	B6 Iab	4.78 ± 0.22	$45.0^{10.1}_{-8.3}$	13.5 ± 1.0	1.75 ± 0.1	$-7.30^{+0.24}_{-0.24}$	250 ± 75	2
HD 91024	B7 Iab	4.74 ± 0.22	$50.0^{-11.4}_{-9.1}$	12.5 ± 1.0	1.95 ± 0.1	$-7.00^{+0.24}_{-0.24}$	225 ± 68	2
HD 199478	B8 Iae	5.08	68.0	13.0 ± 1.0	1.70	-6.70...-6.15	230	4
HD 94367	B9 Ia	4.97 ± 0.22	$77.0^{+17.3}_{-14.1}$	11.5 ± 1.0	1.55 ± 0.1	$-6.62^{+0.24}_{-0.24}$	175 ± 53	2
HD 202850	B9Iab	4.59 ± 0.22	54.0	11.0 ± 1.0	1.85	$-7.22^{+0.26}_{-0.18}$	240	4
HD 212593	B9 Iab	4.79 ± 0.22	59.0	11.8 ± 1.0	2.18	$-7.05^{+0.25}_{-0.17}$	350	4
BP Cru	B1 Ia$^+$	5.67	70.0	$18.1^{+0.5}_{-0.5}$	2.38	-5.00	305	5
ζ^1 Sco	B1.5 Ia$^+$	5.93	103.0	17.2 ± 0.5	1.97	-5.2	390 ± 50	6
HD 190603	B1.5 Ia$^+$	5.58	63.0	18.0 ± 0.5	2.10	-5.66	485 ± 50	6
Cyg #12	B3-4 Ia$^+$	6.28	246.0	$13.7^{+0.8}_{-0.5}$	$1.70^{+0.08}_{-0.15}$	-4.82	400^{+600}_{-100}	6
AG Car	LBV	$6.17^{+0.04}_{-0.05}$	58.5	22.8 ± 0.5	-	$-4.22^{+0.11}_{-0.16}$	300 ± 30	7
		$6.00^{+0.04}_{-0.05}$	115.2	14.3 ± 0.5	-	$-3.92^{+0.11}_{-0.16}$	150 ± 30	7
P Cygni	LBV	5.85	76.0	19.2	-	-4.49	185	8
HR Car	LBV	5.70	70.0	17.9	-	-4.85	120	9
Pistol star	LBV	6.20	306	11.8 ± 1.5	-	-4.12	105	10
FMM 362	LBV	6.25	350	11.3 ± 1.5	-	-4.37	170	10
AFGL2298	LBV	6.30	385	11.0 ± 0.5	-	-4.28	125	11
NS4	WNLh	5.58	22.6	28.4	-	-4.35	700	12
HD 313846	WNLh	5.82	33.1	27.7	-	-4.53	1170	12
GC AF	WNLh	5.3 ± 0.2	28.1 ± 0.6	21.0	-	−4.25 ± 0.2	700 ± 100	13
GC IRS16C	WNLh	5.9 ± 0.2	63.9	19.5 ± 6.0	-	−4.65 ± 0.2	650 ± 100	13
GC IRS34W	WNLh	5.5 ± 0.2	35.9	19.5 ± 6.0	-	−4.88 ± 0.2	650 ± 100	13
GC IRS33E	WNLh	5.75 ± 0.2	63.9	18.0 ± 6.0	-	−4.80 ± 0.2	450 ± 100	13
GC IRS19NW	WNLh	5.9 ± 0.2	59.1	17.5 ± 6.0	-	−4.95 ± 0.2	600 ± 100	13